Cell

Identification of a Targeting Factor for Posttranslational Membrane Protein Insertion into the ER

Sandra Stefanovic[1] and Ramanujan S. Hegde[1,*]
[1] Cell Biology and Metabolism Branch, National Institute of Child Health and Human Development, National Institutes of Health, Room 101, Building 18T, 18 Library Drive, Bethesda, MD 20892, USA
*Correspondence: hegder@mail.nih.gov
DOI 10.1016/j.cell.2007.01.036

SUMMARY

Hundreds of proteins are anchored in intracellular membranes by a single transmembrane domain (TMD) close to the C terminus. Although these tail-anchored (TA) proteins serve numerous essential roles in cells, components of their targeting and insertion pathways have long remained elusive. Here we reveal a cytosolic TMD recognition complex (TRC) that targets TA proteins for insertion into the ER membrane. The highly conserved, 40 kDa ATPase subunit of TRC (which we termed TRC40) was identified as Asna-1. TRC40/Asna-1 interacts posttranslationally with TA proteins in a TMD-dependent manner for delivery to a proteinaceous receptor at the ER membrane. Subsequent release from TRC40/Asna-1 and insertion into the membrane depends on ATP hydrolysis. Consequently, an ATPase-deficient mutant of TRC40/Asna-1 dominantly inhibited TA protein insertion selectively without influencing other translocation pathways. Thus, TRC40/Asna-1 represents an integral component of a posttranslational pathway of membrane protein insertion whose targeting is mediated by TRC.

INTRODUCTION

A fundamental problem in biology is the insertion of proteins into biological membranes. This problem is further complicated in eukaryotic cells by an extensive array of intracellular organelles that necessitates highly selective targeting to one among many membrane systems. For membrane protein biogenesis at the ER, the most well-studied mechanism is a cotranslational insertion pathway mediated by the cytosolic signal recognition particle (SRP), the ER-localized SRP receptor (SR), and an ER protein translocon whose central channel is formed by the Sec61 complex (Shan and Walter, 2005; Osborne et al., 2005). These basic components are highly conserved from bacterial to mammalian systems and are demonstrated to play an essential role in the biosynthesis of a wide range of membrane proteins.

Although ubiquitous, this cotranslational SRP-dependent pathway is inaccessible to a large class of membrane proteins whose only targeting information is encoded in a single transmembrane domain (TMD) close to the C terminus (Kutay et al., 1993; Wattenberg and Lithgow, 2001; Borgese et al., 2003; High and Abell, 2004). These tail-anchored (TA) proteins are released from the ribosome before the TMD emerges from the ribosomal tunnel (which shields ~30–40 residues), precluding cotranslational targeting and translocation. TA proteins are surprisingly abundant in various membrane systems of the eukaryotic cell and play critical roles in nearly all aspects of cell biology (Borgese et al., 2003). Notable examples include the SNAREs involved in vesicular trafficking, several components of translocons in various organelles, components of membrane-bound degradation machinery, structural proteins for Golgi morphology, and numerous enzymes whose activities are spatially restricted in the cell. Despite this broad functional importance of TA proteins, the pathways by which they are targeted to or inserted into the ER membrane remain very poorly understood.

With some exceptions (such as cytochrome b5 [Cb5]), most ER-targeted TA proteins are thought to be inserted via an energy-dependent process that involves at least one proteinaceous component of the ER. Early reconstitution studies suggested convincingly that components of the ER other than the minimal cotranslational machinery (SR, Sec61, and translocating chain-associating membrane protein [TRAM]) were necessary for insertion of the model TA protein synaptobrevin (Kutay et al., 1995). Since that time, a variety of studies have confirmed an ATP requirement for several other TA proteins, provided further support for yet unidentified membrane factors, and characterized some of the sequence requirements for TMD insertion (Kutay et al., 1995; Whitley et al., 1996; Kim et al., 1997, 1999; Steel et al., 2002; Borgese et al., 2001; Abell et al., 2003). These biochemical analyses were buttressed with studies in yeast showing that various mutants in the known co- or posttranslational

translocation pathways are not impaired in TA protein insertion (Steel et al., 2002; Yabal et al., 2003). While recent crosslinking analyses were used to suggest interactions between TA proteins and components of the SRP and Sec61 pathways (Abell et al., 2003, 2004), the functional relevance of these observations remains largely uncertain and in contradiction to previous studies arguing against a role for these components (e.g., Kutay et al., 1995). Thus, the main consensus from the sum of the available studies is that components in the cytosol and membrane, at least one of which may be dependent on ATP, are involved in insertion. However, the identity of the ATP-requiring component(s), the membrane receptor(s), and their mechanisms of action have long remained elusive.

Clarification of these issues will require identification of components in the pathway of insertion. A major obstacle to achieving this goal has been the heterogeneity of insertion assays that rely on measuring membrane binding of TA proteins. A binding assay can contribute significant background noise by not reliably distinguishing a physiologically relevant membrane-spanning orientation from other modes of membrane association, insertion, or aggregation. Hence, the small dynamic range, low throughput, and low sensitivity of this assay have precluded significant attempts at identification of components involved in either targeting or insertion. Recently, this obstacle was overcome by a protease protection assay that not only showed high sensitivity and specificity, but could be employed in combination with fractionation of the lysate components (Brambillasca et al., 2005). This approach greatly facilitated a detailed analysis of Cb5 insertion by the spontaneous pathway (defined here as not requiring any protein factors in the membrane). This study revealed a previously unappreciated ER dependence on lipid composition for insertion of Cb5. Exploiting this advance in methodology, we have now dissected the more broadly utilized, but poorly understood, nonspontaneous TA insertion pathway to identify a key cytosolic component of a TMD recognition complex (TRC) that functions in posttranslational membrane protein targeting. Our results delineate the principal steps in posttranslational membrane protein insertion, allow us to propose a working mechanistic framework for this ubiquitous and physiologically important pathway, and explain how the TRC- and SRP-dependent pathways operate in parallel without cross-interference.

RESULTS AND DISCUSSION

TA Protein Insertion by an Energy-Dependent Protein-Requiring Pathway

The requirements for transmembrane insertion of a model TA protein were analyzed in vitro. The ER translocon component Sec61β was chosen because it is unambiguously inserted solely into the ER, is not trafficked elsewhere, is definitively confirmed to fully span the membrane (as opposed to a hairpin topology), and is highly conserved and universally expressed (Hartmann et al., 1994; Toikkanen et al., 1996; Van den Berg et al., 2004). Hence, Sec61β insertion almost certainly utilizes a general and widely applicable ER-selective pathway whose components are likely to be found in all cells, making its analysis in heterologous in vitro systems physiologically relevant.

Using a recently developed protease protection assay (see Figure S1A in the Supplemental Data), an epitope-tagged Sec61β (referred to hereafter as just Sec61β; see Table S1 in the Supplemental Data) synthesized in a reticulocyte lysate was found to insert posttranslationally into ER-derived rough microsomes (RMs). Correct transmembrane orientation was verified by recovery of a protease protected fragment (PF) representing the epitope-tagged transmembrane segment (Figures 1A and 1B). The PF was not observed when RMs were omitted, if detergent was included in the protease digestion reaction, or if the TMD was deleted from Sec61β (Figures 1A and 1B; Figures S1B and S1C). The choice of epitope tag did not influence the insertion (Figure S1C), and the PF was confirmed in sedimentation assays to cofractionate with RMs (data not shown). Quantitation by phosphorimaging (after accounting for methionine distribution) showed better than 50% absolute insertion efficiency.

Using the generation of PF as a diagnostic marker for correct transmembrane orientation, Sec61β insertion was shown to occur at temperatures above 24°C, was complete within 15 min at 32°C, and was stimulated significantly by an energy regenerating system (Figures 1B and 1C). Using a panel of previously characterized fractionated proteoliposomes and liposomes (see Table S2), we analyzed the membrane requirements for Sec61β insertion. These experiments showed that Sec61β inserts efficiently into proteoliposomes reconstituted from total ER membrane proteins (rRM), but not liposomes (Figure 1D; Figures S1C–S1E) or protease-digested proteoliposomes (Figure 1E). This contrasted with Cb5, whose spontaneous transmembrane insertion into liposomes (or protease-digested proteoliposomes) appears to occur by a pathway not available to Sec61β (Figures 1D and 1E, and Figures S1D and S1E; Brambillasca et al., 2005).

Analyses in various fractionated proteoliposomes (Figure 1F; Table S2) suggested that depletion of known translocon components by ~95% or more was without effect on Sec61β insertion. These depletions included the Sec61 complex, TRAM, the TRAP complex, Sec62, Sec63, oligosaccharyl transferase, and signal peptidase complex. Conversely, proteoliposomes containing only the SR and Sec61 complex failed to support Sec61β insertion even though they were competent for cotranslational translocation of Prl and posttranslational insertion of Cb5 (Figure 1D). Furthermore, modification of free cysteines on the ER membrane (which inhibits cotranslational translocation by modification of the SR; Andrews et al., 1989) had no effect on Sec61β insertion (Figure 1G) despite complete blockage of cotranslational translocation (Figure 1H). Considered together, these findings

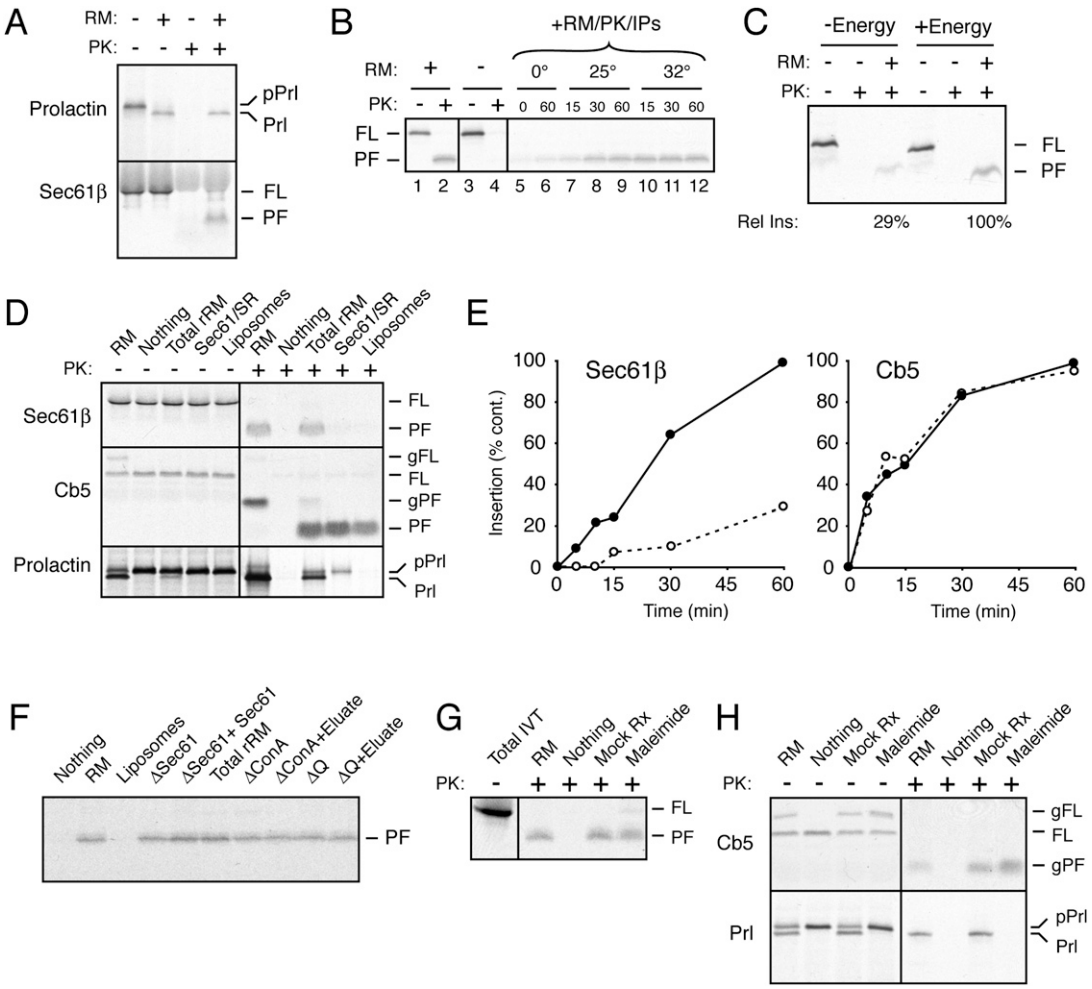

Figure 1. Characterization of a Posttranslational Membrane Protein Insertion Pathway

(A) Prolactin and Sec61β were synthesized in vitro for 30 min at 32°C with or without ER-derived rough microsomes (RM) and analyzed by a protease protection assay (Figure S1A) using proteinase K (PK). The precursor (pPrl) and processed (Prl) forms of Prolactin are indicated, as are the full length (FL) and protected fragment (PF) species of Sec61β. The diffuse band just above Sec61β is hemoglobin from the reticulocyte lysate.

(B) Lanes 1–4 are immunoprecipitates (against a C-terminal epitope tag; see Figure S1A) of translocation reactions as in (A). Lanes 5–12 are Sec61β translation products (without RMs, as in lane 3) that were posttranslationally incubated with RMs at the indicated temperatures for between 0 to 60 min before analysis by PK digestion and immunoprecipitation to recover the PF.

(C) Sec61β translated without RM was isolated by immunoaffinity chromatography (to remove free nucleotides), and the eluted products were tested for insertion into RM in the absence or presence of an energy regenerating system. Quantification by phosphorimaging showed ~3-fold increased insertion with energy.

(D) Cotranslational translocation of Prl and posttranslational insertion of Sec61β and Cb5 were tested with the indicated membrane vesicles (see Table S2) using a protease protection assay. This Cb5 construct (see Table S1) has a glycosylation site at the C terminus that is modified upon insertion into RM (and to a small extent, in rRM). The lack of Prl processing in Sec61/SR proteoliposomes is due to the absence of signal peptidase.

(E) Time course (at 25°C) of Sec61β and Cb5 insertion into rRM (solid lines) or rRM-PK (reconstituted from PK-digested ER membrane proteins).

(F) Posttranslational insertion of Sec61β was tested with the indicated membrane vesicles (see Table S2). Only the protease-digested, immunoprecipitated samples are shown.

(G and H) RM treated with Biotin-maleimide (to modify exposed sulfhydryls) and mock-treated RM was tested for cotranslational translocation of Prl and posttranslational insertion of Sec61β and Cb5. In addition to protease protection, Cb5 insertion and Prl translocation can also be observed by their glycosylation and signal cleavage, respectively.

demonstrate that like synaptobrevin (Kutay et al., 1995), insertion of Sec61β occurs by an energy-stimulated, protein-dependent, posttranslational mechanism that appears to be distinct from the known cotranslational or spontaneous insertion pathways.

Detection of a Cytosolic Targeting Complex for TA Protein Insertion

To find potential components involved in TA protein insertion, we took an unbiased approach utilizing a combination of fractionation, crosslinking, and functional insertion

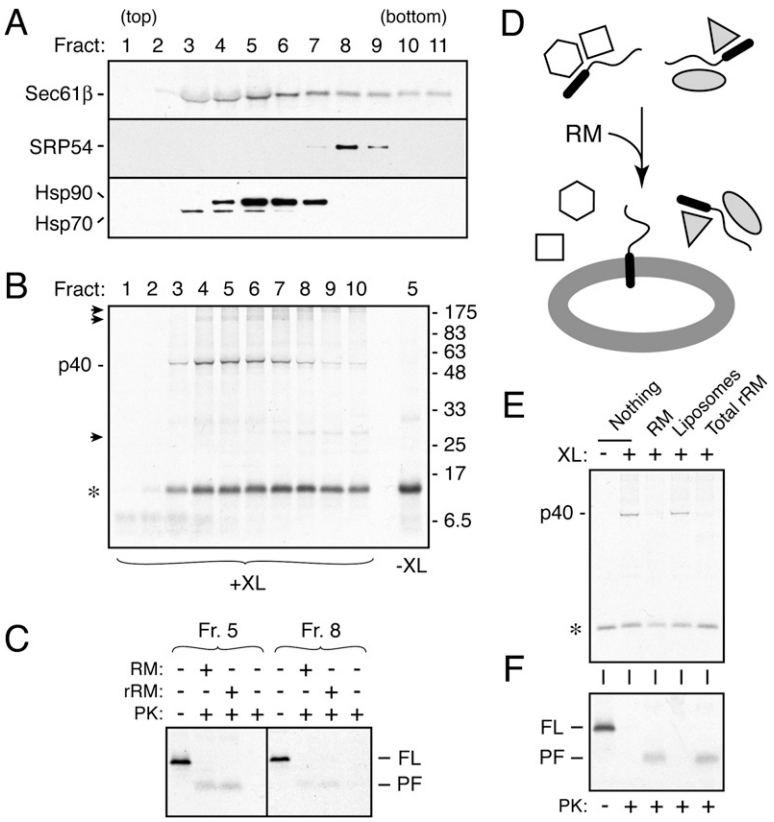

Figure 2. Detection of a Targeting Factor for Posttranslational Membrane Protein Insertion

(A) Sec61β translated in reticulocyte lysate was fractionated using a sucrose velocity gradient and detected by autoradiography. SRP54, Hsp70, and Hsp90 were detected in the same samples by immunoblotting. The distortion of Sec61β in lanes 3 and 4 is comigrating hemoglobin.

(B) Individual fractions from a gradient similar to (A) were treated with BMH, a sulfhydryl reactive crosslinker (XL). Fraction 5 in the absence of crosslinker is shown for comparison. The major crosslinking partner (p40), minor crosslinks (arrowheads), and uncrosslinked Sec61β (*) are indicated.

(C) Fractions 5 and 8 from a gradient as in (A) were tested for insertion into RM and rRM. Phosphorimaging showed ~2.5-fold higher insertion efficiency in fraction 5.

(D) Diagram of expectations for the fate of cytosolic Sec61β-containing complexes that are (left) or are not (right) intermediates on the pathway of membrane insertion.

(E and F) In-vitro-synthesized Sec61β was incubated for 30 min at 32°C with the indicated vesicles, divided in two, and analyzed by either crosslinking (E) or protease protection (F). Note the disappearance of p40 crosslinks only in the samples where insertion has occurred.

analyses. We reasoned that during targeting, TA protein substrates are likely to engage a targeting complex that, at the very least, prevents exposure of the hydrophobic TMD to the aqueous environment. Indeed, sucrose velocity gradient analyses (Figure 2A) of in-vitro-synthesized Sec61β at a step prior to the addition of RMs showed it to be in very heterogeneous complexes ranging from ~4 S to 11 S (roughly ~100 to more than 500 kDa). Formation of these complexes was dependent on the TMD, but was not influenced by the presence or placement of epitope tags (Figure S2A and data not shown).

Analysis of each fraction by chemical crosslinking revealed a variety of crosslinking partners, the most prominent of which was an ~40 kDa protein found largely in fractions 4 through 7 (Figure 2B). These crosslinks were observed with various concentrations of both lysine- and cysteine-reactive crosslinkers, not seen with Sec61β lacking the TMD, and not influenced by the choice or location of epitope tags (Figures S2B and S2C). Importantly, the peak fractions containing this crosslink were clearly separated from peak fractions containing SRP (in which crosslinks to SRP54 were not detectable; Figure S2D). The interaction with p40 was highly sensitive to detergent (Figure S2E), but relatively stable in the presence of elevated salt (to ~250 mM; data not shown), suggesting predominantly hydrophobic-based interactions consistent with involvement of the substrate's TMD.

The peak p40-containing fraction displayed noticeably higher efficiency of insertion when compared with the peak SRP-containing fraction (Figure 2C), suggesting the possibility that the p40-Sec61β complex is an insertion-competent intermediate. To test this idea, we performed crosslinking analyses before and immediately after incubation with membrane vesicles. We reasoned that a bona fide intermediate complex would disassemble concomitant with insertion, whereas off-pathway complexes would be maintained as a noninserted population (Figure 2D). Crosslinks between Sec61β and p40 disappeared concomitant with membrane insertion into either RM or rRM, but not after incubation with insertion-incompetent liposomes (Figures 2E and 2F). Other crosslinks were observed to remain unchanged regardless of membrane incubations (Figure S2F), suggesting that these (relatively minor) interactions represent populations of Sec61β that are not on the productive insertion pathway. Based on the TMD-dependent interaction with Sec61β at a step before (but not after) insertion, we hypothesized that p40 may represent a component of a TA protein-targeting machinery that we have termed TRC. This 40 kDa component, which will be the focus of the remainder of this study, will subsequently be called TRC40.

Identification and Characterization of TRC40 as a Component of TRC

To identify TRC40, we affinity-purified the in-vitro-generated Sec61β-TRC complex (Figure 3A) using anti-peptide antibodies directed against the extreme N terminus of Sec61β under conditions predetermined to preserve

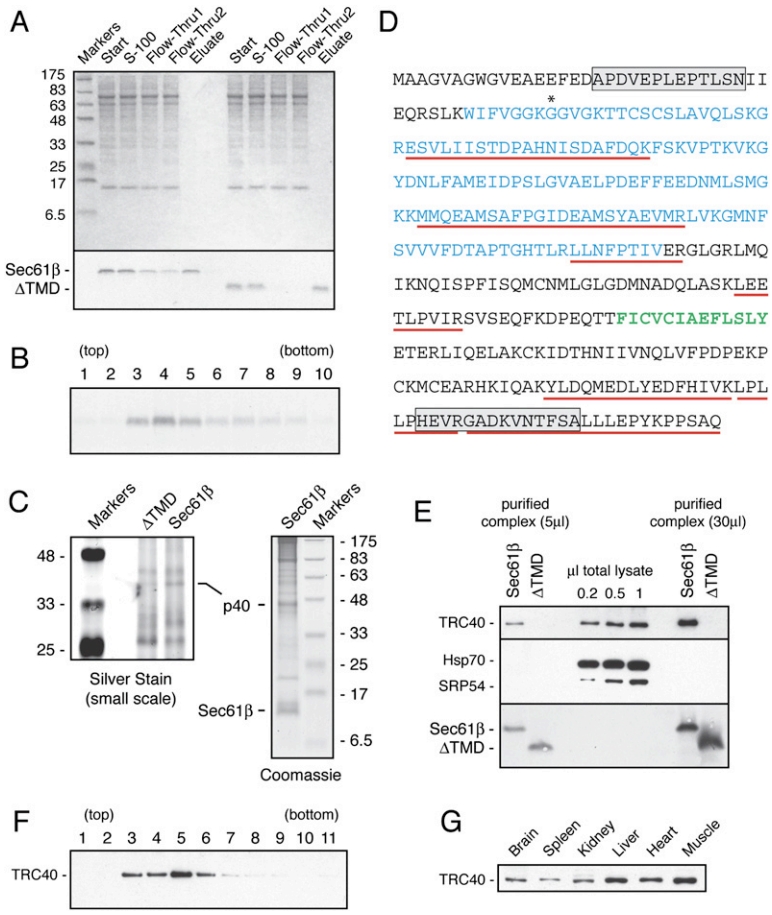

Figure 3. TRC40 Is an ATPase Involved in Posttranslational Membrane Protein Targeting

(A) Sec61β and Sec61β(ΔTMD) were translated in vitro and isolated by immunoaffinity purification under native conditions. The top and bottom panels show the Coomassie-stained gel and autoradiograph, respectively, of samples taken at each step in the purification.

(B) Sucrose velocity gradient analysis of immunoaffinity-purified Sec61β (from A) shows a sedimentation profile similar to the starting sample (compare to Figure 2A) and distinct from constructs lacking the TMD (Figure S2A).

(C) Immunoaffinity-purified Sec61β and Sec61β(ΔTMD) were analyzed by silver staining (left panel). Sample from a ~20-fold larger scale preparation of Sec61β was also analyzed by Coomassie staining (right). The positions of p40 and Sec61β (verified by mass spectrometry) are indicated.

(D) Sequence of TRC40. Tryptic peptides obtained by mass spectrometry are underlined, peptides used for raising antibodies are boxed, the ATPase domain is in blue, and a conserved hydrophobic patch in the C-terminal region is green. (*) indicates the glycine mutated to generate the ATPase-deficient mutant used in Figure 6.

(E) Immunoblots for TRC40, SRP54, and Hsp70 of immunoaffinity-purified Sec61β and Sec61β(ΔTMD) complexes prepared as in (A). Different amounts of reticulocyte lysate (0.2 to 1 μl) were included on the same gel as the purified complexes derived from 5 μl and 30 μl of translation reactions to estimate yield. An autoradiograph to confirm equal recovery of the translation products is shown in the bottom panel.

(F) Fractions from a sucrose gradient similar to Figure 2A were probed with antibodies against TRC40.

(G) The indicated mouse tissues were analyzed by immunoblotting with antibodies against TRC40.

integrity of the complex. Upon peptide-elution under physiologic conditions, the recovered material was confirmed by sucrose gradient analyses (Figure 3B) to still be in similarly sized complexes as before, to display similar crosslinking patterns (data not shown), and importantly, to insert into RM in an energy-stimulated manner (data not shown; cf. Figure 1C). Comparison of the affinity-purified complex to a parallel sample using Sec61β lacking the TMD revealed a TMD-specific ~40 kDa band by silver staining (Figure 3C).

Large-scale translations were subjected to the same procedure and the ~40 kDa product (recovered in a roughly 1:1 stoichiometry with Sec61β; Figure 3C) was identified by mass spectrometry of the tryptic digests. Seven independent peptide fragments matched the predicted sequence for a 348 amino acid protein that contains a highly conserved N-terminal ATPase domain and a C-terminal region containing a conserved hydrophobic patch (Figure 3D; Figures S3A and S3B). This protein was originally annotated Asna-1 in mammals due to ~27% homology to a bacterial ATPase (ArsA) involved in arsenite transport (Kurdi-Haidar et al., 1996). However, these and subsequent authors have found little or no arsenite-stimulated ATPase activity (Kurdi-Haidar et al., 1998; Mukhopadhyay et al., 2006), and conclude that the mammalian protein plays a different role than its distant bacterial homolog. Although knockout of Asna-1 in mice results in early embryonic lethality (Mukhopadhyay et al., 2006), its function has remained unknown. Based on our functional results below, we propose the name TRC40 for this protein.

Two synthetic peptides from the predicted sequence of TRC40 were used to raise antibodies that confirmed the specific presence of TRC40 in the affinity-purified

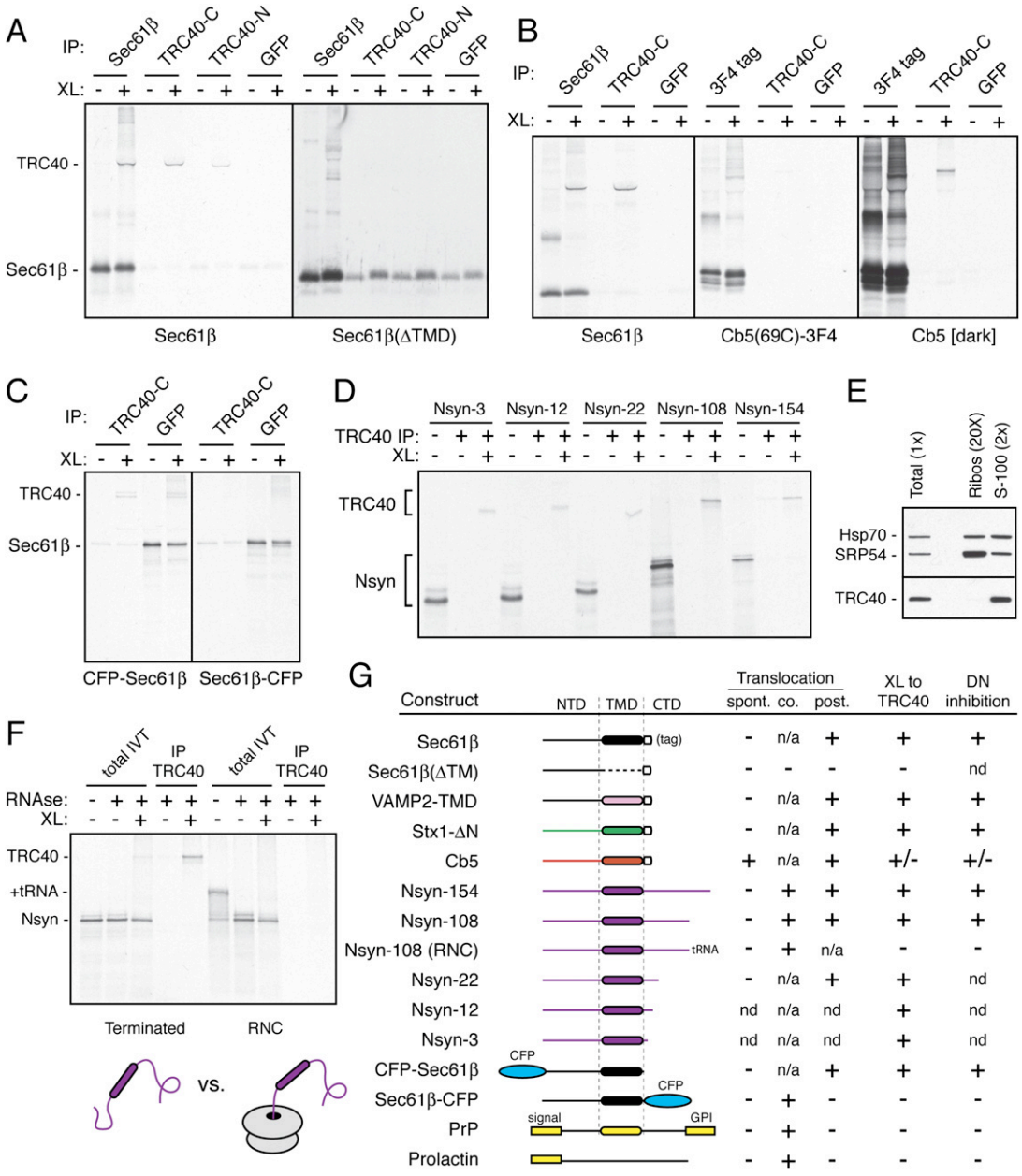

Figure 4. Substrate Specificity of TRC40 for Posttranslational Membrane Protein Insertion

(A) In vitro translation reactions of Sec61β and Sec61β(ΔTMD) were treated with the sulfhydryl reactive crosslinker and immunoprecipitated under denaturing conditions using the indicated antibodies. Anti-GFP served as a nonspecific antibody control. In other experiments, the preimmune sera from the anti-TRC40 rabbits was used as a specificity control with identical results. The Sec61β(ΔTMD) autoradiograph is intentionally overexposed to illustrate complete lack of crosslinks to TRC40.

(B) Constructs encoding Sec61β or Cb5(69C)-3F4, each containing a single cysteine in a comparable position, were analyzed in parallel by crosslinking and immunoprecipitation for interaction with TRC40. The weak crosslink between Cb5(69C)-3F4 and TRC40 could be observed only on longer exposures (right).

(C) CFP-Sec61β and Sec61β-CFP were analyzed in parallel for crosslinking to TRC40. The double band is likely a consequence of crosslinks between different residues.

(D) The indicated Nsyn1 constructs containing tails of various lengths from 3 to 154 residues were analyzed by crosslinking and immunoprecipitation of TRC40. No systematic differences among these constructs in crosslinking efficiencies to TRC40 were observed.

(E) Reticulocyte lysate was separated into ribosomal and soluble (S-100) fractions that were analyzed by immunoblots for TRC40, SRP54, and Hsp70. Ten-fold more ribosomes relative to S-100 were analyzed.

(F) Nsyn-108 was either synthesized completely (terminated) or made as a ribosome-nascent chain complex (RNC), both of which were analyzed by crosslinking. Samples were either analyzed directly ("total") or after immunoprecipitation for TRC40. The indicated samples were treated with RNase

Sec61β-TRC complex (Figure 3E). Of particular importance, TRC40 was not observed in parallel samples using Sec61β lacking the TMD. Neither Hsp70 nor SRP54 were found in appreciable quantities in the Sec61β-TRC complex (Figure 3E and Figure S3C; see Supplemental Data). Furthermore, both the N- and C-terminal anti-TRC40 antibodies could specifically immunoprecipitate the Sec61β-TRC40 crosslink, while neither nonspecific antibodies nor the preimmune sera was able to do so (Figure 4A; data not shown). Finally, immunoblotting revealed that TRC40 migrates in the position of the sucrose gradient in which the 40 kDa crosslinks were most prominently observed (Figure 3F; compare with Figure 2B). Thus, the identified TRC40 protein is indeed the prominent 40 kDa crosslinking partner of TA proteins observed in Figure 2.

As expected for a component of a general TA protein targeting complex, TRC40 is highly conserved in all eukaryotes (Figure S3A; comparable to the level of Sec61α conservation) and appears to be expressed universally in all tissues and cultured cell lines examined so far (Figure 3G). Our conservative estimate for the abundance of TRC40 in reticulocyte lysate is at least ~20–50 nM, several-fold higher than the estimated abundance of cytosolic SRP (~5–10 nM). Because the migration of TRC40 in the sucrose gradient was unchanged in the presence or absence of Sec61β, its assembly into the larger TRC would seem to not be induced by a TA substrate. This supposition was supported by specific crosslinks between TRC40 and several other reticulocyte lysate proteins that were maintained through various fractionation procedures (Figures S3D and S3E). While the identification of the additional component or components await complete purification of native TRC, these results allow us to conclude that TRC40 is one component of a larger preassembled complex that interacts with Sec61β in a TMD-dependent manner prior to its insertion into the ER membrane.

Selectivity of TRC40 Interactions with TA Protein Substrates

Several TA and non-TA proteins were analyzed by crosslinking and immunoprecipitation for their interaction with TRC40 (summarized in Figure 4G). This analysis revealed that deletion of the TMD from Sec61β completely abolished any detectable interaction with TRC40 (Figure 4A), while other TA proteins that are inserted by a nonspontaneous posttranslational pathway (Figure S4A) were readily crosslinked to TRC40 (Figure S5 and data not shown). By contrast, interaction of TRC40 with the spontaneously inserting Cb5 was markedly reduced relative to Sec61β (Figure 4B). Importantly, no interactions could be detected with the cotranslational translocation substrates Prolactin (Prl) or the prion protein (PrP) despite the fact that these proteins contain hydrophobic domains (Figure S5). Both contain an N-terminal signal sequence, and PrP additionally contains an internal (potential) membrane spanning domain and C-terminal hydrophobic domain used for glycosylphosphatidylinositol (GPI) anchor addition. Thus, even though Prl, PrP, and Cb5 are observed by sucrose gradient analyses to be in high molecular weight complexes in the cytosol (data not shown), these complexes do not seem to include TRC40 as a principal interacting component. This suggested that TRC40-substrate interactions are more selective than simple hydrophobicity, and pointed to a context-dependent TMD-mediated interaction.

To test this idea directly, we examined TRC40 interactions with Sec61β constructs appended with cyan fluorescent protein (CFP) at either the N or C terminus (termed CFP-Sec61β and Sec61β-CFP, respectively). Although both constructs are inserted into the ER membrane, Sec61β-CFP is strictly cotranslational, while CFP-Sec61β is inserted posttranslationally (Figure S4B). Remarkably, TRC40 crosslinks were selectively observed with CFP-Sec61β (Figure 4C), even though both constructs contain identical sequence elements, including the TMD. Thus, TRC40 displays selectivity not only for certain TMDs, but also for the context in which these TMDs are found.

However, the contextual cue or cues appear to be more complex than simply a TMD at the C terminus. This became evident when we analyzed a member of the syntaxin family (most of which are TA proteins) from *Neurospora crassa* (Nsyn1) that had evolved an unusually long 154 residue C-terminal tail (Gupta et al., 2003). Nsyn1 constructs containing tails ranging from 3 to 154 residues (termed Nsyn-3 through Nsyn-154) all showed essentially identical crosslinking efficiency to TRC40 (Figure 4D). While this would seem to be at odds with the Sec61β-CFP result above, it could be explained by our observation that Nsyn-108 and Nsyn-154 are capable of posttranslational insertion despite their unusually long tails (Figure S4C). When considered together, these findings reveal a striking relationship between a substrate's interaction with TRC40 and its ability to be integrated into the ER by the nonspontaneous posttranslational membrane protein insertion pathway. We therefore suggest that TRC40 has a context-dependent specificity for TMDs in membrane proteins that utilize this posttranslational pathway of insertion. While this pathway is most widely used by TA proteins that cannot access the cotranslational insertion pathway, it seems that at least some substrates that ordinarily would

immediately prior to SDS-PAGE to remove any attached tRNA. The peptidyl-tRNA in the RNC sample verified that Nsyn-108 was ribosome associated at the time of crosslinking.

(G) Summary of all TRC40 crosslinking analyses and functional properties of various constructs. Schematic representations of constructs are shown and aligned by their relative TMD position. Spontaneous insertion is defined as the ability to insert into liposomes (e.g., Cb5 in Figure 1D). DN inhibition refers to the ability of a TRC40 dominant-negative protein to inhibit insertion (see Figure 6). n/a indicates not applicable (e.g., TA proteins cannot insert cotranslationally and an RNC cannot be tested posttranslationlly), and nd indicates not done.

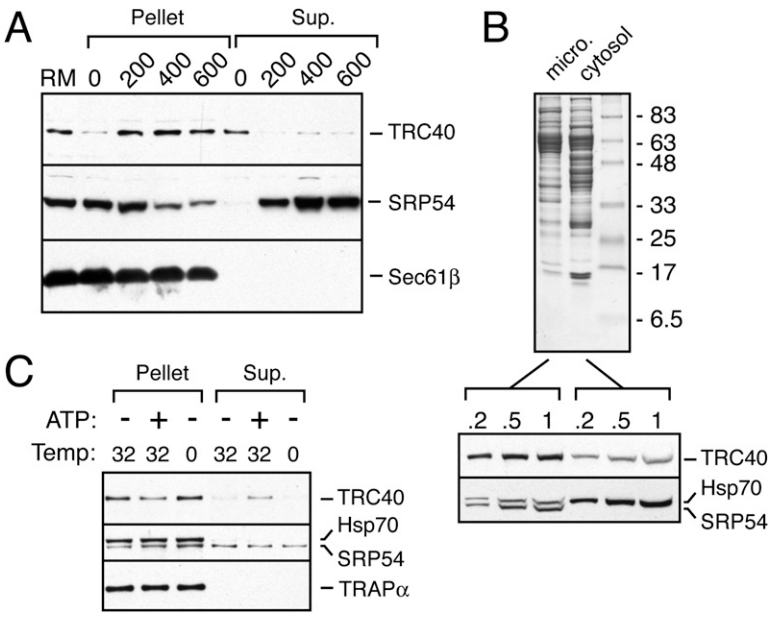

Figure 5. TRC40 Associates Peripherally with the ER Membrane

(A) RM (lane 1) was diluted into hypotonic or hypertonic buffer and recovered by sedimentation. Equal portions of the supernatants and membrane pellets were analyzed by immunoblotting for the indicated products. The dilution buffer contained 250 mM sucrose, 50 mM HEPES (pH 7.4), and 0, 200, 400, or 600 mM KAc as indicated. SRP is a known peripheral protein removed by high salt, while Sec61β serves as an integral membrane protein control.

(B) Microsomes and cytosol from bovine liver were analyzed by Coomassie staining (top) or immunoblotting (bottom).

(C) Liver microsomes were incubated for 10 min under physiologic conditions (100 mM KAc, 50 mM HEPES [pH 7.4], 2 mM $MgAc_2$) at the indicated temperatures in the presence or absence of 1 mM ATP before separation into soluble and membrane fractions and analysis by immunoblotting.

use the SRP pathway (e.g., Nsyn1, which is not formally a TA protein) can also take advantage of the TRC pathway under some circumstances.

Hierarchical Interactions of Membrane Proteins with SRP and TRC40

The ability of TRC40 to interact with a substrate (Nsyn1) containing an internal TMD raised the issue of precisely when and where TRC40 first engages substrate relative to the other principal TMD recognition factor, SRP. Since the TMD of Nsyn1 would emerge from the ribosome long before reaching its termination codon, it is feasible in this instance for TRC40 to bind the nascent (i.e., ribosome-associated) polypeptide. Even for a C-terminal TMD, binding might occur as it emerges from the ribosomal exit tunnel (e.g., if TRC were positioned there) to prevent exposure of the TMD to the aqueous cytosolic environment.

To examine these ideas, we first examined the localization of TRC40 in reticulocyte lysate. Unlike either SRP or Hsp70 (both of which are known nascent chain binding proteins; Krieg et al., 1986; Frydman et al., 1994), TRC40 was not found in association with ribosomes to any appreciable degree (Figure 4E). This raised the possibility that interaction of TRC40 with substrates occurs only upon complete release from the ribosome into the cytosol. Indeed, Nsyn-108 was found in a complex with TRC40 after termination of translation, but not while it was a nascent peptidyl-tRNA bound to ribosomes (at which step other crosslinks were seen; Figure 4F). This result indicates that when hydrophobic domains such as TMDs first emerge from the ribosome, they are likely to be preferential substrates for SRP. This is because the signal recognition cleft of SRP is poised at the ribosomal exit tunnel, effectively creating a very high local concentration (Halic et al., 2004). Upon release from the ribosome, however, a suitably positioned TMD (i.e., in the context of a TA protein) is now a far better substrate for interaction with TRC. This is probably a combination of both a higher free cytosolic concentration of TRC relative to SRP and possibly a higher affinity of interaction in the nonribosomal context. We conclude from the above analyses that upon release of a TMD-containing protein from the ribosome, it is preferentially recognized by TRC, while ribosome-associated nascent chains containing TMDs are preferentially recognized by SRP. Thus, these two complexes, which can recognize TMDs, do not interfere or compete with each other for substrate.

Reversible Binding of TRC40 to the ER Membrane

A key role for a putative targeting factor such as TRC would be its regulated binding and release from membranes competent for insertion of TA proteins. Indeed, immunoblots revealed that RMs contain substantial amounts of peripherally associated TRC40 that can be extracted by low salt, high pH (11.5), urea (2M), or small amounts of detergent (Figure 5A and data not shown). Fractionation of liver under physiologic conditions suggested that at steady state, ~30%–60% of TRC40 is bound to membranes (Figure 5B). Notably, a significant amount of this membrane-bound population of TRC40 could be released from the membrane under physiologic conditions upon brief (10 min) incubation with ATP (Figure 5B). This raised the possibility that the ATPase activity of TRC40 might play a role in the putative TRC targeting cycle. Thus, in addition to being free in the cytosol, endogenous TRC40 can also be found in a membrane-bound form that may represent association with a membrane-localized receptor. Consistent with this idea, in-vitro-synthesized TRC40 was observed to bind ER membranes, but not liposomes (data not shown).

ATPase-Dependent Transfer of TA Proteins from TRC40 to the ER Membrane

The transient interaction of TRC40 with both TA proteins and a putative ER-localized receptor pointed to a possible targeting function in which TRC delivers its substrates for subsequent membrane insertion. Attempts to demonstrate this proposed functional role by immunodepletion of TRC40 were hindered because neither of our anti-TRC40 antibodies recognized the native protein. We therefore took another approach. The energy dependence of TA protein insertion (Kutay et al., 1995; Figure 1C), together with the observations that TRC40 is an ATPase whose membrane binding is influenced by ATP (Figure 5C), suggested to us a model in which ATP hydrolysis coordinates the targeting step (analogous to the use of GTPases in the SRP-dependent targeting pathway). We therefore reasoned that if TRC40 indeed plays a direct role in targeting, an ATPase-deficient mutant may act to dominantly and selectively inhibit TA protein insertion.

A glycine to arginine point mutant in the highly conserved ATP binding pocket of TRC40 (shown previously to disrupt ATPase activity; Shen et al., 2003) was recombinantly expressed, purified, and added at submicromolar concentrations to various translocation reactions. While this mutant (termed TRC40-DN, for dominant-negative) had no effect on cotranslational translocation of Prl (Figure 6A), it dose-dependently inhibited the posttranslational insertion of Sec61β and other TA proteins (Figure 6A). When added to posttranslational translocation reactions of signal sequence-containing α-factor across yeast microsomes (Figure 6B), TRC40-DN had no effect (except a slight nonspecific effect on translation at the highest concentrations). Furthermore, TRC40-DN had only a modest effect on the spontaneously inserting Cb5 substrate (Figure 6C). Considered together, these results indicate that the ATPase-deficient TRC40 dominantly inhibits the principal TA protein insertion pathway without substantial effects on the known cotranslational (Gorlich and Rapoport, 1993), posttranslational (Panzner et al., 1995), or spontaneous (Brambillasca et al., 2005) translocation pathways. These functional effects correlated well with the crosslinking results (Figure 4G): those substrates that interact with TRC40 are inhibited by the ATPase mutant, while substrates like Prl that do not interact with TRC40 are not inhibited. The partial effect on Cb5 is again consistent with its apparently weak interaction with TRC40 (Figure 4B) and its access to the alternate spontaneous insertion pathway (Brambillasca et al., 2005).

The high level of TRC40 selectively for only the posttranslational membrane insertion pathway was analyzed in another way by examining Nsyn-108, a substrate that is normally inserted cotranslationally, but is also capable of posttranslational insertion after ribosome release (Figure S4C). Addition of TRC40-DN to cotranslational translocation reactions of Nsyn-108 had little effect on its membrane integration (Figure 6D). By striking contrast, insertion of this same substrate into the same membranes was inhibited potently by TRC40-DN if the reaction was performed posttranslationally. This result argues strongly for the existence of distinct parallel membrane insertion pathways that utilize different subsets of components, among which TRC40 is selectively posttranslational. Identical results were obtained with Nsyn-154 (data not shown).

Based on these findings, we surmised that the mechanism of dominant inhibition was direct binding of TRC40-DN to ribosomally released substrate. Due to deficient ATPase activity, TRC40-DN would prevent substrate targeting to or release at the ER membrane. To test this, we analyzed the interactions between Sec61β and endogenous TRC40 versus exogenously added (and epitope-tagged) TRC40-DN. At a level of TRC40-DN that inhibits TA insertion by ~50%, crosslinks to the endogenous and exogenous proteins were roughly equal (Figures 6E and 6F). Higher levels of TRC40-DN resulted in increased crosslinking (at the expense of endogenous TRC40 crosslinks) that correlated with increased inhibition of Sec61β (Figure 6F). Upon addition of insertion-competent microsomes, Sec61β was released more efficiently from endogenous TRC40 than from exogenous TRC40-DN (Figure 6G). The unreleased TRC40-DN-substrate complex was found by sedimentation assays to be at least partially membrane bound (data not shown), suggesting that targeting may be normal, but ATPase-dependent release and subsequent insertion were blocked. Considered together, these findings suggest that TRC40 interacts directly with substrate, after which it delivers the TA protein to the membrane where its ATPase activity is necessary for substrate release, subsequent insertion, and recycling of TRC for another round of targeting.

A Working Model for TA Protein Insertion

The results in this study have led to the identification of the first component of a poorly characterized but widely used posttranslational pathway of membrane protein insertion. Our subsequent mechanistic analyses of TRC40 delineate a working framework for the principal steps in this targeting and insertion pathway (Figure 7) and identify specific, important directions for future studies.

Based on the sedimentation (Figure 3F), crosslinking (Figure S3D), and fractionation (Figure S3E) analyses, TRC40 appears to be preassembled into the larger cytosolic TRC even in the absence of substrate. While this complex can be membrane bound (Figure 5), at least half of TRC appears to be free in the cytosol, awaiting ribosome-released TMD-containing substrates. This places TRC "second in line" behind SRP for TMD interaction. The affinity of SRP for ribosomes (Ogg and Walter, 1995) and its positioning relative to the ribosomal exit tunnel (Halic et al., 2004) provides a competitive advantage for nascent chain interactions. This advantage is lost upon translational termination, since TMD-containing polypeptides released into the cytosol appear to be preferentially bound to non-SRP-containing complexes (Figure 2B and Figures S2C and S2D), the principal one of which is TRC (whose abundance also appears to be greater than

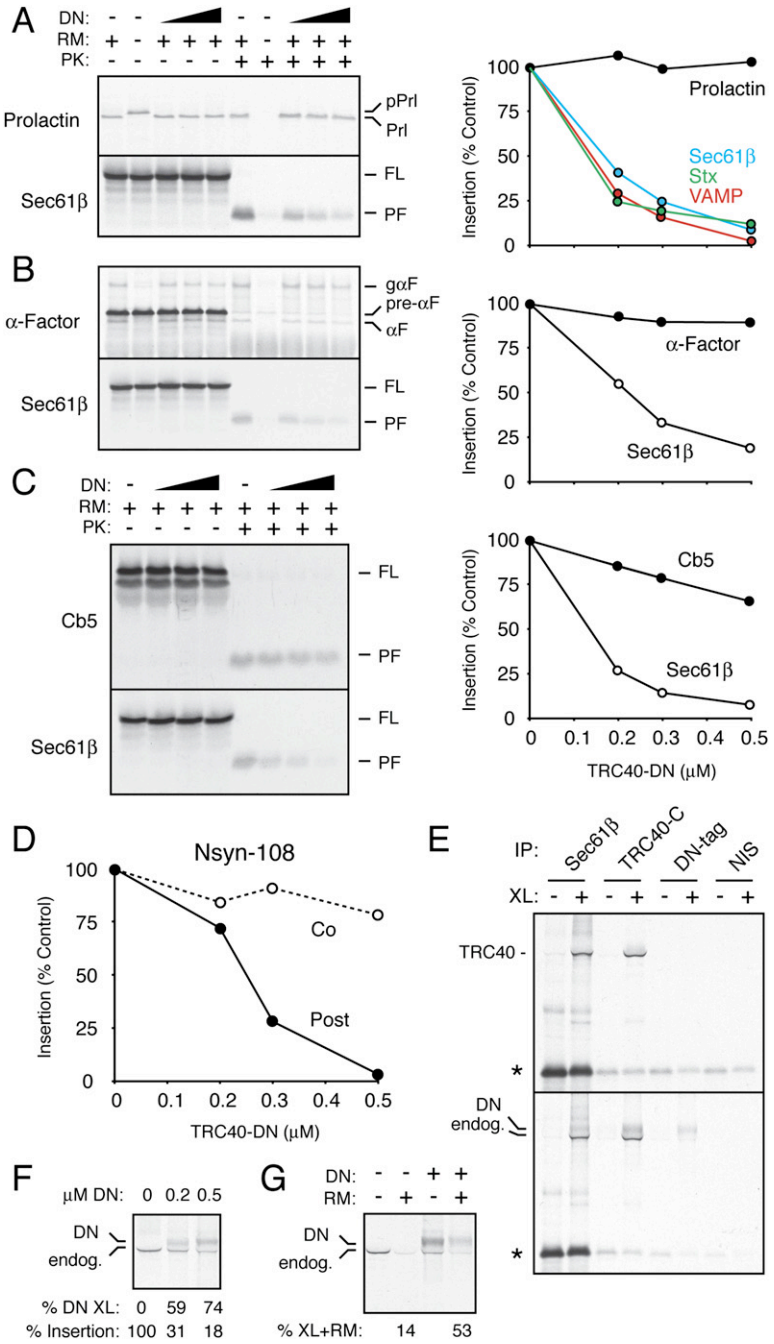

Figure 6. An ATPase Mutant of TRC40 Selectively Inhibits TA Membrane Protein Insertion

(A–C) The indicated proteins were synthesized in the presence of increasing concentrations (from 0 to 0.5 μM) of recombinant TRC40-DN (containing a glycine to arginine mutation at position 46 in the Walker A box) and analyzed for translocation by the protease protection assay. For Prl translocation, RMs were included during the translation reactions, while the other translocation reactions were performed post-translationally. Graphs to the right of each representative experiment show the average of between two and five independent replicates. Yeast RMs were used in (B).

(D) Nsyn-108 was translated in the presence of increasing concentrations of recombinant TRC40-DN, analyzed for translocation by the protease protection assay, and quantified by phosphorimaging. In one set of reactions, RMs were included during translation to permit cotranslational translocation (open symbols), while the other reactions were performed post-translationally using fully synthesized, ribosome-released Nsyn-108 (closed symbols).

(E) Sec61β translated in the absence (top) or presence (bottom) of 0.2 μM TRC40-DN was analyzed by crosslinking and immunoprecipitation with antibodies against Sec61β, TRC40, the tag on TRC40-DN, or an irrelevant antibody (NIS). The slower migration of TRC40-DN crosslinks relative to endogenous TRC40 is due to the epitope tag, and the diffuseness of this band is caused by comigrating IgG heavy chain.

(F) Sec61β translated in the presence of the indicated concentration of TRC40-DN was subjected to crosslinking and immunoprecipitation with anti-TRC40. The relative crosslinking to exogenous TRC40-DN (as a percent of total TRC40 crosslinks) is indicated below the gel, as are the relative insertion efficiencies at the respective TRC40-DN concentrations.

(G) Crosslinking analysis of Sec61β translated in the presence of 0.5 μM TRC40-DN before and after incubation with RM. The percent of total TRC40 crosslinks remaining after RM incubation was quantified by phosphorimaging and is indicated below the gel. Note that release from TRC40-DN is relatively poor upon incubation with RM when compared with release from endogenous TRC40.

SRP's in reticulocyte lysate). How TRC out-competes chaperones such as Hsp70 remains unclear. One possibility is that while Hsp70 binds and releases from substrates in an ATPase-driven cycle (Mayer and Bukau, 2005), the TRC40-substrate interaction is stable until its delivery to the membrane (e.g., Figure S2E). Thus, we favor a model in which TRC acts as a "trap" to sequester cytosolic TMD-containing substrates from other potential interacting partners that may serve to temporarily prevent substrate aggregation.

The mechanism underlying the specificity of TRC for TMDs remains to be determined. However, two points are worth noting. First, simple hydrophobicity is not likely to be the sole determinant since substrates containing a signal sequence, C-terminal GPI-anchoring signal, or a spontaneously inserting TMD were all poor substrates for TRC interaction, and were also not significantly inhibited by TRC40-DN (Figure 4G). Second, the interaction of TRC is not limited solely to TMDs at the extreme C terminus (Figure 4D). Thus, the TRC-dependent pathway

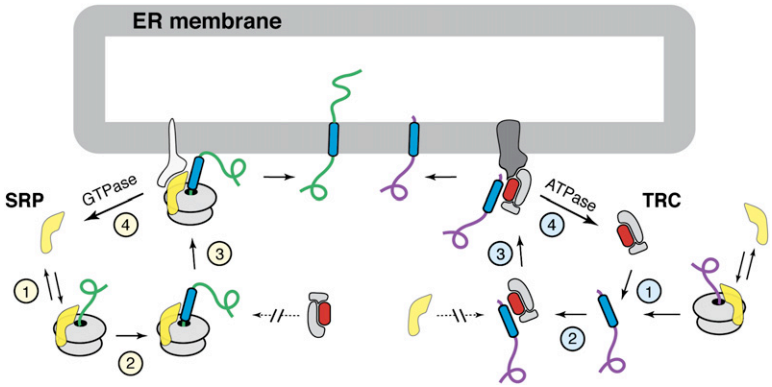

Figure 7. Model for the Role of TRC40 in Posttranslational Membrane Protein Insertion

The cotranslational SRP pathway (left) is compared with the posttranslational pathway (right) mediated by the multicomponent TRC (whose ATPase TRC40 subunit is shown in red). The basic steps of substrate synthesis (1), recognition of the TMD (2), receptor-mediated targeting to the ER membrane (3), and nucleotide hydrolysis-dependent substrate release (4) are indicated in each pathway. The posttargeting step of TMD insertion is not depicted. The two pathways do not interfere or compete with each other due to the distinct mechanisms of SPR versus TRC function (see text for details). Thus, the substrate clienteles (and membrane-bound machinery) for the TRC- and SRP-dependent pathways are proposed to be distinct. Only certain unusual TA proteins with long tails would be capable of using both systems.

may be utilized by not only TA proteins, but also membrane proteins that, for one reason or another, missed their opportunity to target via the SRP-dependent pathway. Of course, the TRC pathway presumably has many additional constraints and would fail to insert complex membrane proteins or those whose intended lumenal domains had already folded (such as Sec61β-CFP; Figure 4C). But our demonstration that Nsyn1, with a tail of 154 residues, can not only interact with TRC40 (Figure 4D) but also be inserted posttranslationally (Figure S4C) provides one example of a membrane protein that can insert by both co- and posttranslational pathways that utilize different machineries and operate in parallel.

Once bound to a TMD-containing substrate in the cytosol, TRC presumably interacts with a putative receptor at the ER membrane. This interaction does not appear to be dependent on engaging a substrate since in-vitro-synthesized TRC40 can bind ER microsomes (data not shown). Furthermore, native ER microsomes contain prebound TRC40. Binding of substrate to TRC may enhance its interaction with the membrane receptor, but this needs to be further explored. An analogy to the SRP targeting system is applicable here: while SRP has an affinity for both empty ribosomes and its ER-bound receptor, the presence of a nascent chain substrate (and nucleotide) substantially enhances these interactions to favor efficient targeting without substantial competition by free SRP. We envisage an analogous situation for TRC (Figure 7).

Release of substrate from TRC at the membrane is dependent on the ATPase activity of TRC40. At least three reactions must occur at this step. First, the ATPase activity of TRC40 is presumably stimulated by its receptor interaction. Second, substrate must be released from TRC40 upon ATP hydrolysis. Third, the released TMD must then either be inserted directly into the membrane or transferred to an "insertase" that mediates membrane integration of the TMD and translocation of the tail. It seems unlikely that insertion is "spontaneous" upon release from TRC40 given that even large regions of up to 154 residues can be translocated simultaneously with insertion. The simplest model is that the putative receptor for TRC40 carries out all three activities by stimulating the TRC40 ATPase, binding to the substrate released from TRC40, and serving as the insertase.

Recently, the homolog of TRC40 in *S. cerevisiae* (termed Arr4 or Get3) has been implicated in a variety of processes, including Golgi-to-ER trafficking, ER-associated degradation, sporulation, regulation of ion transport, and tolerance to certain stresses (Shen et al., 2003; Schuldiner et al., 2005; Metz et al., 2006; Auld et al., 2006). The relationship between these phenotypes in yeast and our demonstrated role of mammalian TRC40 in TA protein insertion remains unclear at present. One explanation is that Arr4/Get3 has a functional role or roles in yeast that are distinct from and unrelated to the TA insertion pathway. Alternatively, the conclusion by Auld et al. (2006) that all of these phenotypes are connected in some way to intracellular membrane composition and organization raises the possibility that partial defects in TA protein insertion might underlie some or all of these pleiotropic effects. If this were the case, one would have to postulate that another insertion pathway or pathways can compensate to a large degree in yeast (since Arr4/Get3 deletion is not lethal), but not in mammals, where disruption of TRC40 shows early embryonic lethality (Mukhopadhyay et al., 2006). Development of quantitative assays for TA protein insertion of multiple substrates in the yeast system will be needed to investigate these questions in depth and determine the extent to which the machinery of this translocation pathway is conserved across diverse species.

Toward this end, it is clear that identification of the complete TRC, as well as the membrane component or components that serve as the putative TRC receptor, represent important future goals. Our discovery of TRC40 as a central ATPase that coordinates the targeting and membrane insertion reactions should now greatly facilitate the purification of other pathway components. Once these are in hand, the process of posttranslational membrane protein insertion can be reconstituted with purified components to fully dissect its mechanistic basis.

EXPERIMENTAL PROCEDURES

Materials

All constructs used in this study were made by standard methods and verified by sequencing. The initial cDNA for human TRC40 was obtained from Origene, and Nsyn1 from G. Gupta and B. Heath (Gupta et al., 2003). A complete list of constructs and their composition is provided in Table S1. Rabbit antisera to the N- and C-terminal regions of TRC40 and to the 3F4 epitope were generated by immunizing rabbits with KLH-conjugated synthetic peptides (see Figure 3D and Figure S1A). Antibodies to GFP were raised against recombinant His-tagged GFP (from G. Patterson) expressed from the pRSETA vector in *E. coli*. This antiserum recognizes both the epitope tag and GFP, and was used for either purpose as indicated in the figure legends. Yeast RMs were a gift from T. Rapoport. Bovine liver microsomes and cytosol were prepared by differential centrifugation as for pancreatic RMs (Walter and Blobel, 1983), except homogenization and fractionation was performed in physiologic salt buffer (100 mM KAc, 50 mM HEPES [pH 7.4], 2 mM $MgAc_2$, 250 mM sucrose), and the sucrose cushion for the final centrifugation step was 0.8 M instead of 1.3 M. The sources of published or commercially available materials used in this study are provided in the Supplemental Data.

Insertion and Translocation Assays

Assays for cotranslational translocation (of Prl, PrP, GFP-fusions, and Nsyn1 constructs), posttranslational insertion (of Sec61β, Cb5, and various other TA-proteins), and posttranslational translocation (of α-factor and other proteins) have been described (Fons et al., 2003; Brambillasca et al., 2005; Panzner et al., 1995). In general, co- and posttranslational reactions were for 30 min at 32°C. Unless otherwise indicated, an energy regenerating system (1 mM ATP, 1 mM GTP, 10 mM Creatine phosphate, and 40 μg/ml creatine kinase) was present during the incubation. Posttranslational reactions were generally performed on samples treated with a protein synthesis inhibitor, depleted of ribosomes by centrifugation (70,000 rpms for 30 min in a TL100.3 rotor), or both. Any modifications to these methods are indicated in the figure legends, with additional details provided in the Supplemental Data.

Sucrose Gradient Analyses

Gradients were 5%–25% (w/v) sucrose in physiological salt buffer (PSB; 100 mM KAc, 50 mM HEPES [pH 7.4], 2 mM $MgAc_2$). Sedimentation was for 5 hr at 55,000 rpm in a TLS-55 rotor (Beckman) at 4°C. RNCs were isolated using 10%–50% (w/v) sucrose gradients in PSB spun for 1 hr at 55,000 rpms. Either 10 or 11 fractions were manually collected from the gradients and analyzed directly or subjected to further manipulations (such as crosslinking and insertion assays as described in individual figure legends).

Crosslinking Analyses

Samples for crosslinking (generally taken from the appropriate fraction or fractions of a sucrose gradient) were adjusted to between 20 and 500 μM BMH or DSS (as indicated in the figure legends) added from freshly prepared stocks in DMSO (whose final concentration in the reaction did not exceed 2%). BMH reactions were incubated on ice for 30 min, while DSS was reacted at room temperature for 30 min. Reactions were quenched with 100 mM 2-mercaptoethanol, 100 mM Tris, or both before either direct analysis or further processing (e.g., for immunoprecipitation).

Immunoaffinity Isolation and Identification of TRC40

A 0.2 to 0.5 ml column of anti-Sec61β (against the extreme N terminus) immobilized on Protein A agarose was washed briefly in 0.2 M glycine (pH 2.3) and equilibrated in PSB at 4°C. Translation reactions [either 1 ml (small scale) or 20 ml (large scale)] were depleted of ribosomes by centrifugation and passed over the resin (sometimes up to three times) at 4°C. The column was washed extensively with PSB, and in some cases, with PSB containing 250 mM KAc. Elution was with 1 mM peptide for 30 min at room temperature in PSB. For subsequent sucrose gradients, insertion analyses, or immunoblots, samples were used directly. For analysis by staining or high-sensitivity immunoblots, proteins were concentrated by precipitation with TCA in the presence of 0.5% Triton X-100 carrier, washed in acetone, and dissolved in 1% SDS. Bands were excised from Coomassie-stained gels for tryptic digests and mass spectrometry (performed by Midwest Bio Services).

Recombinant Expression and Purification

Expression in *E. coli* from the pRSETA vector was induced with IPTG, and the His-tagged protein (which was largely insoluble) was purified under denaturing conditions (with 4M urea) using immobilized Ni^{+2} (on chelating sepharose from Amersham). The protein was refolded on the column by washing extensively with PSB and eluted with imidazole in PSB before dialysis against PSB to remove imidazole.

Miscellaneous Methods

Immunoprecipitations in this study were always under denaturing conditions. After samples were heated in 1% SDS to 100°C, they were diluted 10-fold in IP buffer (1% Triton X-100, 50 mM HEPES [pH 7.4], 100 mM NaCl) at 4°C and immunoprecipitated as before (Fons et al., 2003). Most analyses were on 12% Tris-Tricine gels containing 0.1% SDS. Some analyses (Figure 3C, Figures S2C, S2D, and S3D) used 10% Tris-Glycine gels. Immunoblotting utilized nitrocellulose. Optimal antibody dilutions were determined empirically in preliminary experiments. Secondary antibodies were HRP-conjugated. Development was with chemiluminescence reagents from Pierce. Quantification of radiolabeled gels employed the Typhoon phosphorimager system with accompanying software. Figures were made from scanned films using Adobe Photoshop and Illustrator software.

Supplemental Data

The Supplemental Data for this article can be found online at http://www.cell.com/cgi/content/full/128/6/1147/DC1/.

ACKNOWLEDGMENTS

We are grateful for gifts of reagents from G. Gupta, B. Heath, N. Borgese, T. Rapoport, G. Patterson, and P. Roche. We also thank D. Mitra, N. Hegde, and S. Bhat for help in making some of the constructs; M. Hemm and G. Patterson, for advice on recombinant protein purification; A. Sharma, for help with antibody production; H. Bernstein, for useful discussions; and members of the Hegde lab, for advice and support. This work was supported by the intramural research program of the National Institute of Child Health and Human Development at the National Institutes of Health.

Received: November 7, 2006
Revised: December 8, 2006
Accepted: January 5, 2007
Published: March 22, 2007

REFERENCES

Abell, B.M., Jung, M., Oliver, J.D., Knight, B.C., Tyedmers, J., Zimmermann, R., and High, S. (2003). Tail-anchored and signal-anchored proteins utilize overlapping pathways during membrane insertion. J. Biol. Chem. *278*, 5669–5678.

Abell, B.M., Pool, M.R., Schlenker, O., Sinning, I., and High, S. (2004). Signal recognition particle mediates post-translational targeting in eukaryotes. EMBO J. *23*, 2755–2764.

Andrews, D.W., Lauffer, L., Walter, P., and Lingappa, V.R. (1989). Evidence for a two-step mechanism involved in assembly of functional signal recognition particle receptor. J. Cell Biol. *108*, 797–810.

Auld, K.L., Hitchcock, A.L., Doherty, H.K., Frietze, S., Huang, L.S., and Silver, P.A. (2006). The conserved ATPase Get3/Arr4 modulates the activity of membrane-associated proteins in Saccharomyces cerevisiae. Genetics *174*, 215–227.

Borgese, N., Gazzoni, I., Barberi, M., Colombo, S., and Pedrazzini, E. (2001). Targeting of a tail-anchored protein to endoplasmic reticulum and mitochondrial outer membrane by independent but competing pathways. Mol. Biol. Cell *12*, 2482–2496.

Borgese, N., Colombo, S., and Pedrazzini, E. (2003). The tale of tail-anchored proteins: coming from the cytosol and looking for a membrane. J. Cell Biol. *161*, 1013–1019.

Brambillasca, S., Yabal, M., Soffientini, P., Stefanovic, S., Makarow, M., Hegde, R.S., and Borgese, N. (2005). Transmembrane topogenesis of a tail-anchored protein is modulated by membrane lipid composition. EMBO J. *24*, 2533–2542.

Fons, R.D., Bogert, B.A., and Hegde, R.S. (2003). Substrate-specific function of the translocon-associated protein complex during translocation across the ER membrane. J. Cell Biol. *160*, 529–539.

Frydman, J., Nimmesgern, E., Ohtsuka, K., and Hartl, F.U. (1994). Folding of nascent polypeptide chains in a high molecular mass assembly with molecular chaperones. Nature *370*, 111–117.

Gorlich, D., and Rapoport, T.A. (1993). Protein translocation into proteoliposomes reconstituted from purified components of the endoplasmic reticulum membrane. Cell *75*, 615–630.

Gupta, G.D., Free, S.J., Levina, N.N., Keranen, S., and Heath, I.B. (2003). Two divergent plasma membrane syntaxin-like SNAREs, nsyn1 and nsyn2, contribute to hyphal tip growth and other developmental processes in Neurospora crassa. Fungal Genet. Biol. *40*, 271–286.

Halic, M., Becker, T., Pool, M.R., Spahn, C.M., Grassucci, R.A., Frank, J., and Beckmann, R. (2004). Structure of the signal recognition particle interacting with the elongation-arrested ribosome. Nature *427*, 808–814.

Hartmann, E., Sommer, T., Prehn, S., Gorlich, D., Jentsch, S., and Rapoport, T.A. (1994). Evolutionary conservation of components of the protein translocation complex. Nature *367*, 654–657.

High, S., and Abell, B.M. (2004). Tail-anchored protein biosynthesis at the endoplasmic reticulum: the same but different. Biochem. Soc. Trans. *32*, 659–662.

Kim, P.K., Janiak-Spens, F., Trimble, W.S., Leber, B., and Andrews, D.W. (1997). Evidence for multiple mechanisms for membrane binding and integration via carboxyl-terminal insertion sequences. Biochemistry *36*, 8873–8882.

Kim, P.K., Hollerbach, C., Trimble, W.S., Leber, B., and Andrews, D.W. (1999). Identification of the endoplasmic reticulum targeting signal in vesicle-associated membrane proteins. J. Biol. Chem. *274*, 36876–36882.

Krieg, U.C., Walter, P., and Johnson, A.E. (1986). Photocrosslinking of the signal sequence of nascent preprolactin to the 54-kilodalton polypeptide of the signal recognition particle. Proc. Natl. Acad. Sci. USA *83*, 8604–8608.

Kurdi-Haidar, B., Aebi, S., Heath, D., Enns, R.E., Naredi, P., Hom, D.K., and Howell, S.B. (1996). Isolation of the ATP-binding human homolog of the arsA component of the bacterial arsenite transporter. Genomics *36*, 486–491.

Kurdi-Haidar, B., Heath, D., Aebi, S., and Howell, S.B. (1998). Biochemical characterization of the human arsenite-stimulated ATPase (hASNA-I). J. Biol. Chem. *273*, 22173–22176.

Kutay, U., Hartmann, E., and Rapoport, T.A. (1993). A class of membrane proteins with a C-terminal anchor. Trends Cell Biol. *3*, 72–75.

Kutay, U., Ahnert-Hilger, G., Hartmann, E., Wiedenmann, B., and Rapoport, T.A. (1995). Transport route for synaptobrevin via a novel pathway of insertion into the endoplasmic reticulum membrane. EMBO J. *14*, 217–223.

Mayer, M.P., and Bukau, B. (2005). Hsp70 chaperones: cellular functions and molecular mechanism. Cell. Mol. Life Sci. *62*, 670–684.

Metz, J., Wachter, A., Schmidt, B., Bujnicki, J.M., and Schwappach, B. (2006). The yeast Arr4p ATPase binds the chloride transporter Gef1p when copper is available in the cytosol. J. Biol. Chem. *281*, 410–417.

Mukhopadhyay, R., Ho, Y.S., Swiatek, P.J., Rosen, B.P., and Bhattacharjee, H. (2006). Targeted disruption of the mouse Asna1 gene results in embryonic lethality. FEBS Lett. *580*, 3889–3894.

Ogg, S.C., and Walter, P. (1995). SRP samples nascent chains for the presence of signal sequences by interacting with ribosomes at a discrete step during translation elongation. Cell *81*, 1075–1084.

Osborne, A.R., Rapoport, T.A., and van den Berg, B. (2005). Protein translocation by the Sec61/SecY channel. Annu. Rev. Cell Dev. Biol. *21*, 529–550.

Panzner, S., Dreier, L., Hartmann, E., Kostka, S., and Rapoport, T.A. (1995). Posttranslational protein transport in yeast reconstituted with a purified complex of Sec proteins and Kar2p. Cell *81*, 561–570.

Schuldiner, M., Collins, S.R., Thompson, N.J., Denic, V., Bhamidipati, A., Punna, T., Ihmels, J., Andrews, B., Boone, C., Greenblatt, J.F., et al. (2005). Exploration of the function and organization of the yeast early secretory pathway through an epistatic miniarray profile. Cell *123*, 507–519.

Shan, S.O., and Walter, P. (2005). Co-translational protein targeting by the signal recognition particle. FEBS Lett. *579*, 921–926.

Shen, J., Hsu, C.M., Kang, B.K., Rosen, B.P., and Bhattacharjee, H. (2003). The Saccharomyces cerevisiae Arr4p is involved in metal and heat tolerance. Biometals *16*, 369–378.

Steel, G.J., Brownsword, J., and Stirling, C.J. (2002). Tail-anchored protein insertion into yeast ER requires a novel posttranslational mechanism which is independent of the SEC machinery. Biochemistry *41*, 11914–11920.

Toikkanen, J., Gatti, E., Takei, K., Saloheimo, M., Olkkonen, V.M., Soderlund, H., De Camilli, P., and Keranen, S. (1996). Yeast protein translocation complex: isolation of two genes SEB1 and SEB2 encoding proteins homologous to the Sec61 beta subunit. Yeast *12*, 425–438.

Van den Berg, B., Clemons, W.M., Jr., Collinson, I., Modis, Y., Hartmann, E., Harrison, S.C., and Rapoport, T.A. (2004). X-ray structure of a protein-conducting channel. Nature *427*, 36–44.

Walter, P., and Blobel, G. (1983). Preparation of microsomal membranes for cotranslational protein translocation. Methods Enzymol. *266*, 19599–19610.

Wattenberg, B., and Lithgow, T. (2001). Targeting of C-terminal (tail)-anchored proteins: understanding how cytoplasmic activities are anchored to intracellular membranes. Traffic *2*, 66–71.

Whitley, P., Grahn, E., Kutay, U., Rapoport, T.A., and von Heijne, G. (1996). A 12-residue-long polyleucine tail is sufficient to anchor synaptobrevin to the endoplasmic reticulum membrane. J. Biol. Chem. *271*, 7583–7586.

Yabal, M., Brambillasca, S., Soffientini, P., Pedrazzini, E., Borgese, N., and Makarow, M. (2003). Translocation of the C terminus of a tail-anchored protein across the ER membrane in yeast mutants defective in signal peptide-driven translocation. J. Biol. Chem. *278*, 3489–3496.

Cell, volume 128

Supplemental Data

Identification of a Targeting Factor for Posttranslational Membrane Protein Insertion into the ER

Sandra Stefanovic and Ramanujan S. Hegde

Supplementary Note

As shown in Sup. Fig. S3C, SRP54 was in fact detectable at low levels in immunoaffinity isolated complexes of Sec61β. This interaction was TMD-specific and reproducible, consistent with the previous report of weak crosslinks between TA proteins and SRP (Abell et al., 2004). Nonetheless, there are several reasons to believe the interaction with SRP is not likely to represent a substantial or physiologically relevant pathway for insertion of TA proteins. First, our and other functional studies (most notably, Kutay et al., 1995) have failed to detect any consequence of SRP receptor depletion or inactivation on TA protein insertion (e.g., Fig. 1G). Second, the presence in the membrane of SRP receptor and Sec61 complex was insufficient to reconstitute even small amounts of TA protein insertion by the highly sensitive protease protection assay used in this study (Fig. 1D; Kutay et al., 1995). Third, fractions containing SRP were less efficient at insertion than fractions lacking SRP (Fig. 2C). Fourth, crosslinking between a TA protein substrate and SRP54 was either undetectable (our study) or extremely inefficient (Abell et al., 2004). In instances where it was detected (at less than a few percent of total substrate), we would note that a very high crosslinker concentrations (1 mM) was employed at higher temperature (30°C). By contrast, detection of TRC40 crosslinks were readily apparent at all concentrations tested (Sup. Fig. S2C), seen with two different types of crosslinkers, seen with numerous substrates, observed at efficiencies approaching ~20%, and found under very mild conditions (20 μM on ice for 30 min). And finally, direct visualization of all proteins in the Sec61β immunoaffinity purified complex (Fig. 3C; coomassie stained sample) failed to reveal SRP components (except by immunoblot of overloaded samples; Sup. Fig. S3C), while TRC40 was present at near-stoichiometric amounts with Sec61β. In fact, our estimates based on the abundance of SRP in reticulocyte lysate compared with the amount recovered in Sec61β-containing complexes suggest a stoichiometry of less than 1:25 in complex with Sec61β. While we cannot exclude the possibility that SRP *can* mediate TA protein targeting under certain circumstances, it does not appear to contribute significantly under normal circumstances. Thus, the low-level interaction between TA proteins and SRP may be due to the fact that both contain hydrophobic regions.

Supplementary Methods

Materials

In initial experiments and for immunoprecipitation of PrP, mouse monoclonal antibody against the 3F4 epitope was obtained commercially (Signet). Most other experiments used our custom-

made rabbit polyclonal antibody against this epitope. Antibody to the opsin tag on Cb5 was either from N. Borgese or purchased from Sigma. Antibodies to Sec61β and other translocon components have been characterized (Fons et al., 2003; Brambillasca et al., 2005). All other antibodies were obtained commercially: SRP54 (BD Biosciences); Hsp70 and Hsp90 (Stressgen); Prolactin (ICN). Specificity of custom antisera was verified by comparison to the respective pre-immune sera in immunoblotting of whole cell lysates, immunoprecipitation of labeled protein, and peptide competition. Secondary antibodies were from Jackson ImmunoResearch, immobilized Protein A from BioRad, immobilized Protein G from Pierce, Talon immobilized metal resin (for isolation via the His-tag) from Clontech, DEAE- and SP-sepharose from Amersham, and amino-Hexyl agarose from Sigma. Reagents for in vitro transcription, translation in reticulocyte lysate, RMs, liposomes, proteoliposomes, and purified translocon components have been described (Fons et al., 2003; Brambillasca et al., 2005; Garrison et al., 2005). Bismaleimidohexane (BMH), Disuccinimidyl suberate (DSS), and Biotin-maleimide were from Pierce.

In vitro transcription

All templates for in vitro transcription and translation contained either a SP6 or T7 promoter. Transcription reactions containing a 5' cap analogue were for 60 min at either 40°C (for SP6) or 37°C (for T7). The template was either the circular plasmid or PCR products generated by amplification using primers flanking the promoter at the 5' end and termination codon at the 3' end. If a T7 or SP6 promoter was not contained in the plasmid, the appropriate sequence was encoded in the PCR primer. The 3' primer to generate the template for Nsyn1-108 RNCs lacked a stop codon.

In vitro translation, translocation, and protease protection assays

Translation reactions utilized rabbit reticulocyte lysate (RRL) prepared as described (Jackson and Hunt, 1983). In more recent experiments, crude RRL was purchased from Green Hectares, supplemented with Hemin (40 μM), nuclease treated (12 min at 25°C with 150 U/ml micrococcal nuclease), and supplemented with salts (KAc, Hepes, and $MgAc_2$), amino acids (40 μM each except Methionine), calf liver tRNA, and an energy regenerating system for use in translation reactions. Optimal concentrations of each reagent were determined empirically in separate experiments and are available upon request. Aliquots of the complete translation extract lacking ^{35}S-Methionine were frozen in nitrogen and stored at -80°C. Translation was initiated by addition of completed transcription reactions (without further purification) and ^{35}S-Methionine (from MP-Biomedical). Where indicated for co-translational translocation reactions, vesicles were included during the translation. For RMs, the amount used was 1 μl per 10 μl reaction, where the starting RMs were at an A_{280} concentration of 50 [a concentration defined as 1 equivalent (eq) per μl]. Liposomes were usually added at a final concentration of 2 to 5 μg/μl phospholipid (comparable to the amount of phospholipid in the RM-containing reactions). Proteoliposomes were usually added at approximately 3 to 5 eq (as judged by comparative immunoblotting of translocon components relative to RMs) per 10 μl reaction. Unless otherwise indicated, all translation reactions were for 30 min at 32°C, at which point the reactions were generally placed on ice before further manipulations.

For post-translational translocation, one (or both) of two manipulations were performed before addition of vesicles. Either the samples were centrifuged (30 min at 70,000 rpms in microtest tubes with adaptors in the TL100.3 rotor) to remove ribosomes or puromycin was

added to 1 mM. This ensured that all translocation was necessarily post-translational and ribosome-independent. The translation reactions were then incubated with vesicles (at the concentrations described above for co-translational reactions). The standard reaction was for either 15 or 30 min at 32°C, conditions shown in early experiments to achieve maximal translocation/insertion. Samples were then placed on ice for protease protection assays.

Proteolysis was initiated by addition of PK to a final concentration of 0.5 mg/ml. If translation reactions were not in crude lysate, they were always diluted in PSB (i.e., isotonic conditions). Reactions continued for 60 min at 0°C before termination with the addition of PMSF to ~5-10 mM on ice. After 5 min, the sample was then transferred directly to 10 volumes of 1% SDS/0.1 M Tris, pH 8 that was pre-heated in a boiling water bath. Heating continued for at least 2 min after sample addition. Both the PMSF and rapid transfer to boiling SDS were necessary to ensure no inadvertent proteolysis after solubilization. For some experiments, these samples were analyzed directly by SDS-PAGE. Most experiments were subsequently subjected to immunoprecipitation as follows.

After cooling to room temperature, the sample was diluted 10-fold with IP buffer (1% Triton X-100, 100 mM NaCl, 50 mM Hepes, pH 7.4) at 4°C and the antibodies added. In general, polyclonal antisera were used at ~2 to 4 µl per sample. Incubation was for at least 90 min and at most ~16 h. The immunoglobulins were recovered with either Protein A agarose or Protein G agarose (from BioRad and Pierce, respectively), incubated in batch for at least 60 min. In many experiments, the Protein A/G and antibodies were incubated simultaneously. The beads were washed at least three times with IP buffer, eluted with SDS-PAGE sample buffer and analyzed after heating to 100°C. All gels were coomassie stained (or in the case if immunoblots, Ponceau stained) to verify equal loading and/or equal recovery of IgG in all samples.

For the His-tagged constructs (Fig. S1C), products were recovered using Talon beads from Clontech using 0.5x IP buffer instead of 1x IP buffer (which partially inhibits binding). Incubation was for 1 to 2 h, and the beads were washed 3 times with 0.5x IP buffer before elution in SDS-PAGE sample buffer supplemented with 50 mM EDTA.

Crosslinking analyses

All crosslinking reactions were performed on samples that were first fractionated by sucrose gradient sedimentation to separate the protein samples from free reducing agents and primary amine-containing buffers present in the translation reactions. Hence, the first gradient fraction (which contains these small molecules) was never used for crosslinking. Either individual fractions (e.g., Fig. 2B) or pooled fractions containing the radiolabled translation products were used for subsequent crosslinking. While proteins can be more rapidly separated from small molecules using gel filtration/desalting resins, we consistently found this to be less effective and of variable reliability. We later discovered this to be caused by non-specific interactions between many sepharose-based resins and TRC under the native low salt conditions of translation reactions. Non-specific interactions were not a problem for immunoprecipitations, which were under detergent-containing denaturing conditions.

The gradient fractions for crosslinking were either used directly, or in some experiments (e.g., Fig. 2E, 6G, and S2E), first incubated with additional reagents prior to crosslinking. For incubations with vesicles (e.g., RM, rRM, of liposomes), concentrations were the same as those used for the insertion assays above and was for 30 min at 32°C before transfer to ice. Crosslinkers (BMH and DSS) were always prepared fresh from powder by dissolving in DMSO at a concentration at least 25 to 50-fold higher than the intended final concentration (to minimize

the DMSO concentration in the final reaction). We also note that it proved important to replace the crosslinkers regularly (every few months), presumably because moisture inactivates it over time. All BMH crosslinking reactions were performed on ice, while DSS was reacted at room temperature. Reactions were terminated with a vast molar excess (at least 50-fold) of 2-mercaptoethanol and Tris, pH 8.0 before further manipulations. Denaturation was with 1% SDS followed by heating to 100°C. Immunoprecipitation of the denatured products was as described above.

Immunoprecipitations with antibodies against TRC40 were usually performed with a C-terminal antibody that was first affinity purified on immobilized peptide using standard methods. Identical results were obtained with the N-terminal antibody, which in nearly all cases, was included in parallel reactions to validate the specificity of the products. Non-specific controls were either pre-immmune sera from the same rabbit or another polyclonal serum against an irrelevant protein (generally our polyclonal anti-GFP or anti-TRAPα). Specificity controls for monoclonal antibodies employed an irrelevant monoclonal of the same species and class of IgG.

The recombinant TRC40-DN contains an N-terminal tag that consists of a 6His-tag, a T7 epitope, and an enterokinase cleavage site (all part of the pRSETA vector). This tag was selectively recognized by our polyclonal antibodies raised against GFP containing the same tag. Thus, the experiment in Fig. 6E used these GFP antibodies to selectively immunoprecipitate the recombinant TRC40-DN protein.

Crosslinking of endogenous TRC40 to other TRC components

These experiments utilized reticulocyte lysate (or fractions generated from it) and not the translation extracts. This avoids the introduction of amines and sulfhydryl agents that would interfere with crosslinking reactions. Subsequent fractionation was performed using amine-free buffers (Hepes) and without reducing agents. The other aspects of crosslinking were as above and described in the legend to Fig. S3.

Supplementary Table 1. Summary and descriptions of constructs used in this study

Name used in this study	Description of construct
Sec61β	Full length Human Sec61β appended at the C-terminus with the 3F4 epitope (KTNMKHMAGAAA) and no linker amino acids.
Sec61β(ΔTMD)	Identical to Sec61β except residues 68 to 96 coding for the TMD were replaced with the linker residues TG.
His-Sec61β	Full length Human Sec61β appended at the N-terminus with the 6-His epitope in vector pET-19.
His-Sec61β(ΔTMD)	Identical to His-Sec61β except lacking residues 73 to 96 coding for the TMD.
Sec61β-His	Full length Human Sec61β appended at the C-terminus with the 6-His epitope in vector pET-21.
Sec61β(ΔTMD)-His	Identical to Sec61β-His except lacking residues 73 to 96 coding for the TMD.
VAMP2-TMD	Identical to Sec61β(ΔTMD) except the Rat VAMP2 TMD (residues 91 to 114) was inserted at the linker between Sec61β and the 3F4 tag.
Stx1A-ΔN	Rat Syntaxin1A appended at the C-terminus with the 3F4 tag and containing a 212 residue deletion in the N-terminus to shorten the protein. This deletion did not affect the insertion properties of this protein as tested by in vitro assays..
Cb5	Rabbit cytochrome b5 containing a C-terminal opsin tag that contains a site for N-glycosylation. Described in Brambillasca et al., 2005.
Cb5-3F4	Rabbit cytochrome b5 containing a C-terminal 3F4 tag. Confirmed to behave identically to Cb5 using in vitro insertion assays.
Cb5(69C)-3F4	Identical to Cb5-3F4 except residue 69 (a serine) was replaced with cysteine to allow crosslinking analysis with sulfhydryl-reactive agents.
Nsyn-154	Full length syntaxin Nsyn-1 from Neurospora crassa. This contains a C-terminal tail of 154 residues beyond the TMD.
Nsyn-108	A truncated version of Nsyn-154 containing only 108 residue-long tail.
Nsyn-22	A truncated version of Nsyn-154 containing only 22 residue-long tail.
Nsyn-12	A truncated version of Nsyn-154 containing only 12 residue-long tail.
Nsyn-3	A truncated version of Nsyn-154 containing only 3 residue-long tail.
CFP-Sec61β	Full length Human Sec61β appended at the N-terminus with monomeric cyan fluorescent protein (mCFP).
Sec61β-CFP	Full length Human Sec61β appended at the C-terminus with monomeric cyan fluorescent protein (mCFP).
PrP	Full length wild type Hamster Prion protein (PrP).
Prolactin	Full length bovine pre-prolactin.
α-factor	Full length pre-pro-alpha-factor from S. cerevisiae.
His-GFP	Full length green fluorescent protein (GFP) appended at the N-terminus with a 6-His tag, T7 epitope, and enterokinase cleavage site. This tag is from the vector pRSETA.
His-TRC40	Full length human TRC40 in the pRSETA vector as with His-GFP. The tag on this construct is recognized by antibodies raised against the recombinant His-GFP, and were used in immunoprecipitation experiments of Fig. 6E.
TRC40-DN	Identical to His-TRC40 except the glycine at residue 46 in the conserved Walker A box was mutated to arginine.

Supplementary Table 2. Properties of fractionated proteoliposomes.

Vesicles	Components Depleted	Prolactin Transloc.	Cb5 Insertion	PrP Transloc.	Signal Cleavage	Glycosylation	Sec61β Insertion
RM	n/a	+++	+++	+++	+++	+++	+++
Total rRM	lumenal & peripheral proteins	++	+++	+	++	+	+++
rRM-PK	everything except highly PK-resistant proteins	-	+++	-	n/a	-	+/-
Liposomes	everything	-	+++	-	n/a	-	-
ΔSec61	Sec61 complex; partial depl. of some RAMPs	-	+++	-	n/a	+	+++
ΔSec61+ Sec61	Partial depl. of some RAMPs	++	+++	+	++	+	+++
ΔConA	Glycoproteins including TRAM, TRAP, SPC, OST	++	+++	+/-	+/-	-	+++
ΔConA+Eluate	comparable to rRM	++	+++	+	++	+	+++
ΔQ	Highly acidic proteins including TRAP, Sec62, Sec63, OST	++	+++	+/-	++	-	+++
ΔQ+Eluate	comparable to rRM	++	+++	+	++	+	+++

Notes: These data are compiled from experiments shown in Fons et al. (2003), Garrison et al. (2005), Brambillasca et al. (2005) and this study.

"+/-" indicates a detectable, but very small effect. "n/a" indicates not applicable (e.g., signal cleavage cannot be measured without translocation of a signal-containing protein).

All proteoliposomes are depleted of lumenal and peripheral proteins comparable to rRM.

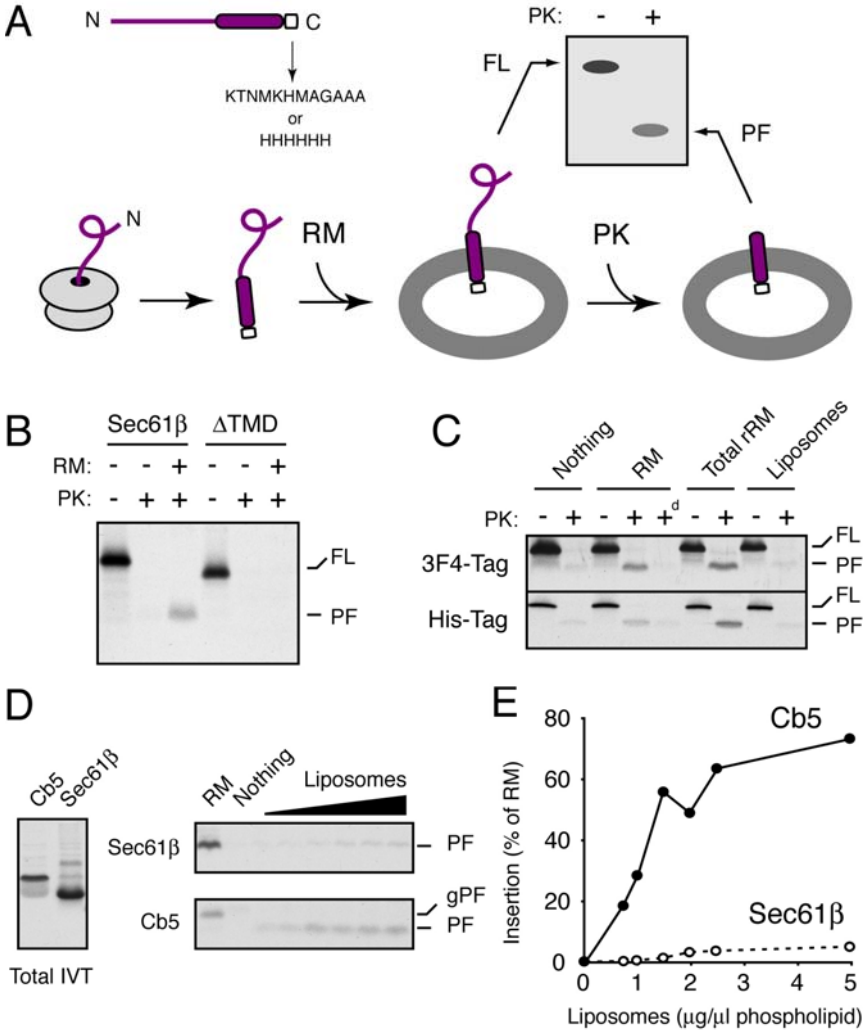

Figure S1. Additional characterization of the pathway for Sec61β insertion. (A) The Sec61β construct used in most of this study is appended at the C-terminus with a 12 residue tag recognized by the 3F4 antibody. Some experiments used a poly-histidine tag to confirm that results were independent of the tag. Upon synthesis, Sec61β is released from the ribosome before the TMD (oval) emerges from the ribosomal tunnel. It is then post-translationally inserted into microsomes, where its correct transmembrane orientation is assayed by a protease protection assay using proteinase K (PK). The full length (FL) and protease protected fragment (PF) containing the epitope tag can be recovered by immunoprecipitation to ensure specificity of the products. (B) Constructs encoding either Sec61β or Sec61β(ΔTMD) (both containing the 3F4 tag) were assayed for post-translational insertion into RM as depicted in panel A. The positions of FL and PF species is indicated. (C) Sec61β constructs containing either the 3F4 or His tag were assayed for insertion using RM, rRM (reconstituted proteoliposomes containing total RM membrane proteins), or liposomes as indicated. The higher background with the His tag is due to incomplete digestion of the TMD-His6 fragment by PK. (D) In vitro translation (IVT) products of either Sec61β or Cb5 (left panel) were incubated for 60 min at 32° C with either RM or increasing concentrations of liposomes before digestion with PK and immunoprecipitation to recover the PF (right panels). The tag on Cb5 (from bovine Opsin) contains a glycosylation site that is utilized upon insertion into RM, but not liposomes (Brambillasca et al., 2005). (E) The insertion efficiencies (relative to RM) from panel D were quantified and plotted. The final concentration of phospholipid added as liposomes in the translocation reaction is indicated on the x-axis.

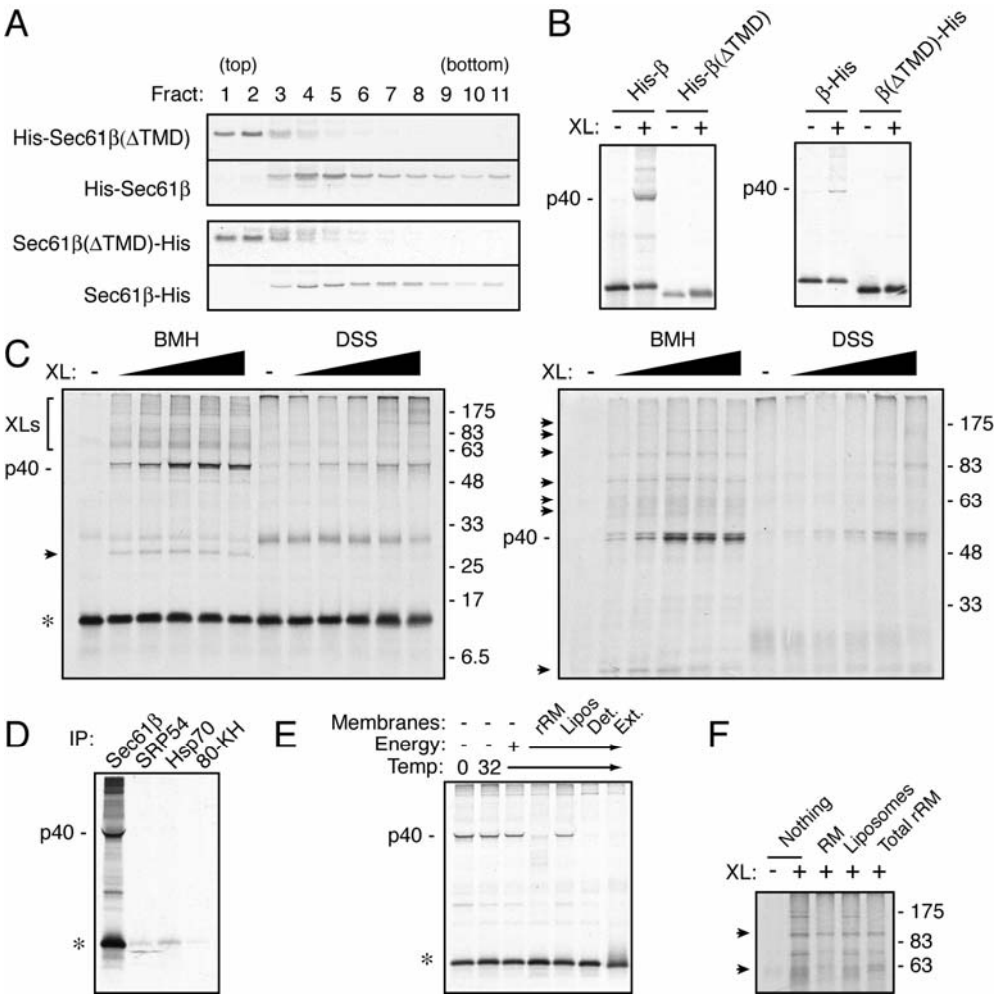

Figure S2. Additional characterization of Sec61β interactions with cytosolic proteins. (A) Sec61β constructs with a 6-His tag at the N- or C-terminus containing or lacking the TMD were translated in vitro and analyzed by sucrose gradient sedimentation as in Fig. 2A. (B) The peak fractions from panel A were analyzed by sulfhydryl-reactive crosslinking. Crosslinking to p40 was the most prominant TMD-dependent interaction. (C) Sec61β (containing the 3F4 tag) was subjected to crosslinking with BMH (sulfhydryl-reactive) or DSS (amine-reactive) at various concentrations (20, 50, 150, 250, and 500 μM) and analyzed on two types of gels to visualize the crosslinks. The most prominent crosslink in all cases was to p40 (which sometimes migrates as a doublet, presumably due to different residues that participate in the crosslinking). Other crosslinks are indicated with arrowheads and uncrosslinked Sec61β with an asterisk. (D) Sec61β crosslinking reaction was immunoprecipitated using the indicated antibodies. The 80-KH antibody (against an ER-lumenal protein) serves as a negative control. (E) In vitro translated Sec61β was incubated under the indicated conditions for 30 min before crosslinking with BMH at 200 μM. Note that incubation with rRM, detergent (0.5% deoxyBigCHAP) or a detergent extract (Ext) of RMs results in release of p40 from Sec61β. (F) Samples from the experiment in Fig. 2E were analyzed on a lower percentage gel and exposed longer to visualize several of the higher molecular weight crosslinks. The arrowheads point to crosslinks that, unlike p40, do not consistently disappear after incubation with insertion-competent vesicles (RM and rRM).

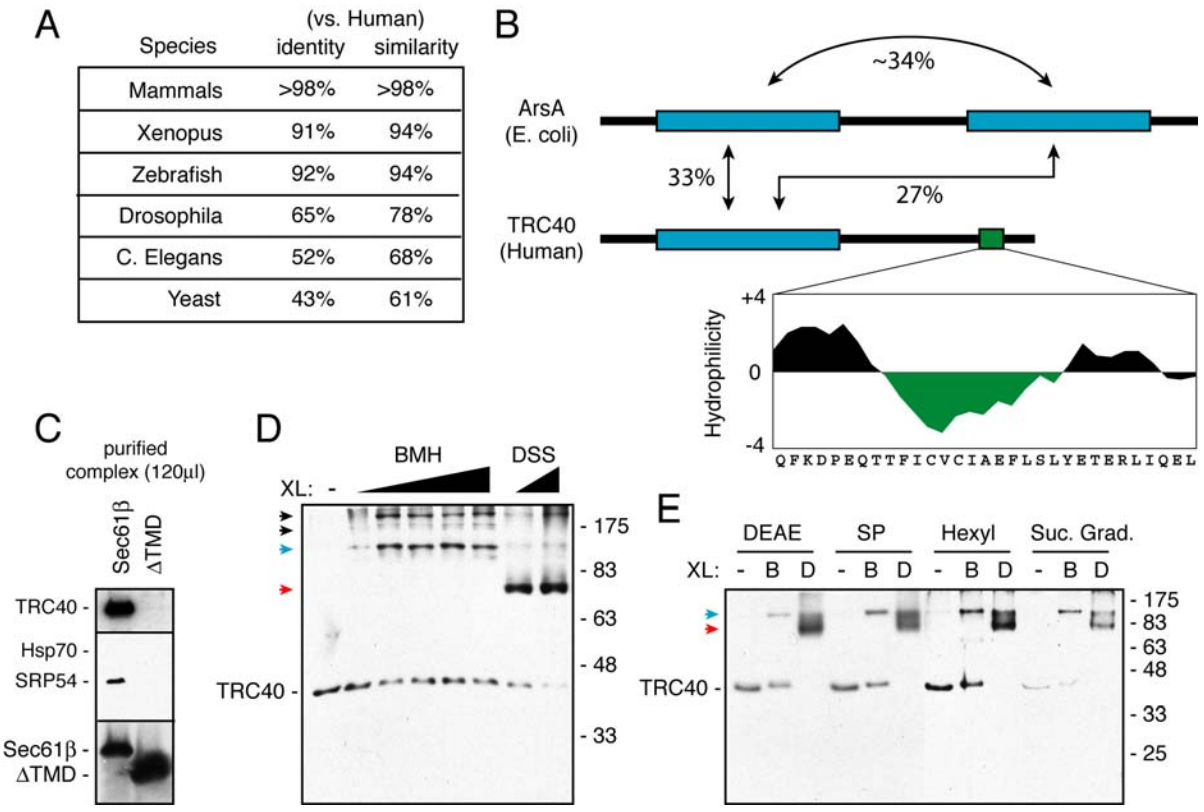

Figure S3. Additional analysis of TRC40. (A) The percent identity and similarity (at the amino acid level) between Human TRC40 and the indicated species are tabulated. ClustalW was used for sequence alignment. As a point of reference, Human and Yeast (S. cerevisiae) Sec61α are 55% identical. (B) Domain structure of ArsA protein from E. coli compared to Human TRC40. ArsA has tandem ATPase domains that are ~34% identical at the amino acid level, while TRC40 has a single ATPase domain that shares ~33% and 27% identity with the ArsA ATPases. In addition, TRC40 has a C-terminal domain that is unique to eukaryotes and contains a conserved hydrophobic/amphipathic region (green). A hydrophobicity plot (using the Kyte-Doolittle scale) of this conserved domain (84% identity and 94% similarity between human and yeast) is shown with the hydrophobic patch in green. (C) A large amount of the samples from Fig. 3E was analyzed by blotting for TRC40, Hsp70, and SRP54. Note that a small amount of SRP54 (equivalent to that found in ~ 0.2 µl of starting lysate) is observed. This corresponds to a recovery of ~0.17% and is 20-40 fold lower yield than TRC40. Given a several-fold higher abundance of TRC40 in reticulocyte lysate, we estimate that on a molar basis, at least 100-fold more TRC40 was recovered in the Sec61β-containing complex than SRP. (D) Reticulocyte lysate was treated with various concentrations (between 10 and 500 µM) of either BMH or DSS and analyzed by immunoblotting for TRC40. Note that TRC40 crosslinks efficiently to proteins of ~35 kD (red arrow), 110 kD (blue arrow), and more than 150 kD (black arrows). (E) Reticulocyte lysate was subjected to fractionation by DEAE-sepharose, SP-sepharose, hydrophobic interaction chromatography (on amino-Hexyl agarose), and sucrose gradient. The fractions containing TRC40 were analyzed by crosslinking with BMH (B) and DSS (D) as in panel D (although the gel type is different). The ~35 kD and ~110 kD crosslinking partners consistently co-fractionate with TRC40 and are indicated with arrows.

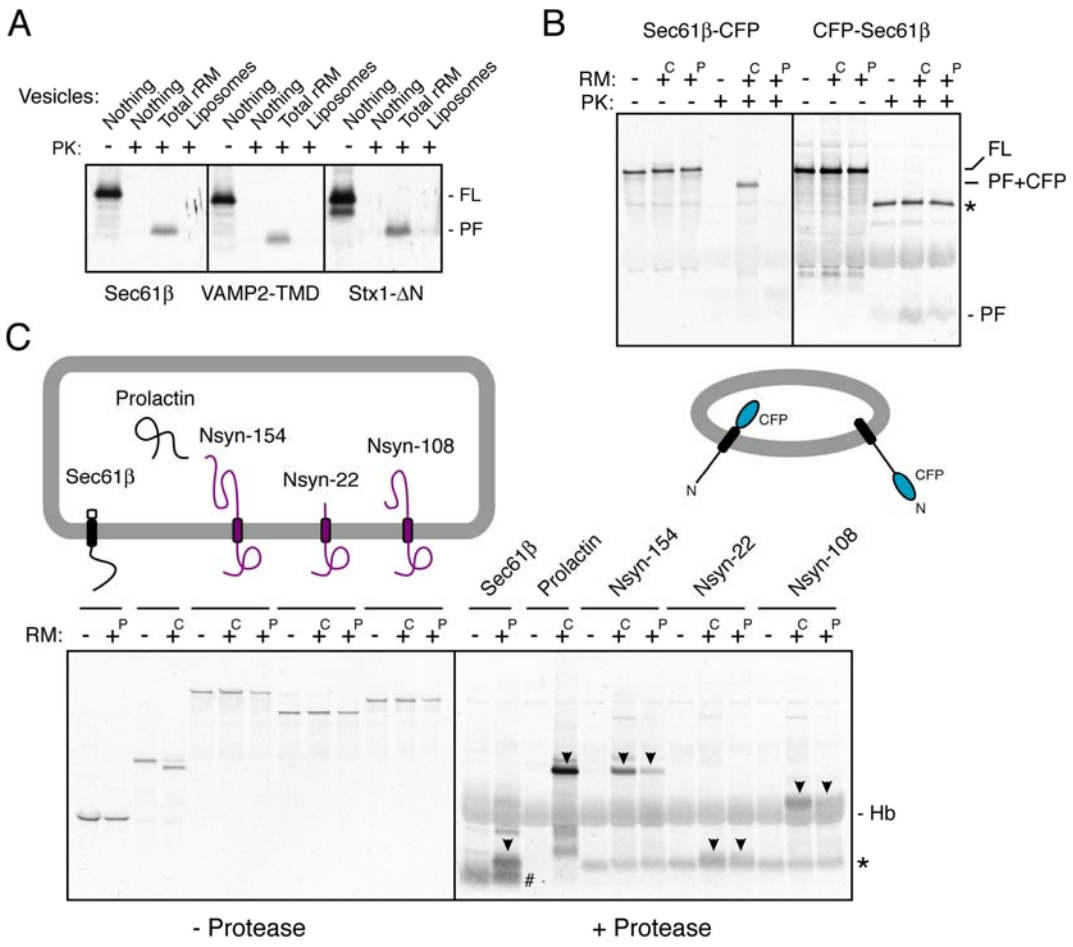

Figure S4. Analysis of various constructs for membrane insertion. (A) The indicated constructs (diagrammed in Fig. 4G) were tested for post-translational insertion into rRM and liposomes as in Fig. 1. In each case, insertion was efficient into rRM, but not detected with liposomes. (B) The CFP-tagged Sec61β constructs were tested for insertion into RM that were either included co-translationally (superscript 'C') or added post-translationally (superscript 'P'). The topology of the constructs is indicated below the autoradiograph. Note that Sec61β-CFP is strictly co-translationally inserted, while CFP-Sec61β can be inserted post-translationally. The CFP-containing PF generated by PK digestion of translocated Sec61β-CFP is indicated ('PF+CFP'), as is the protected fragment (PF) for inserted CFP-Sec61β. The asterisk indicates the position of a protease-resistant core of CFP that is seen in all PK-digested lanes (more prominent for CFP-Sec61β, which is from a longer exposure needed to visualize the PF band). (C) The indicated constructs, diagrammed in their expected topology, were tested for co- and/or post-translational insertion into RM as in panel B. A small aliquot of the synthesized products is analyzed in the left panel, while the remainder was digested with protease and analyzed in the right panel (without immunoprecipitation). The arrowheads indicate the various fragments protected from protease digestion in a membrane-dependent manner. The '*' and '#'indicate terminal digestion fragment of Nsyn and Sec61β. The position of hemoglobin (Hb) is also indicated and is seen in all lanes. Note that the Nsyn constructs are capable of insertion post-translationally despite relatively long C-terminal tails.

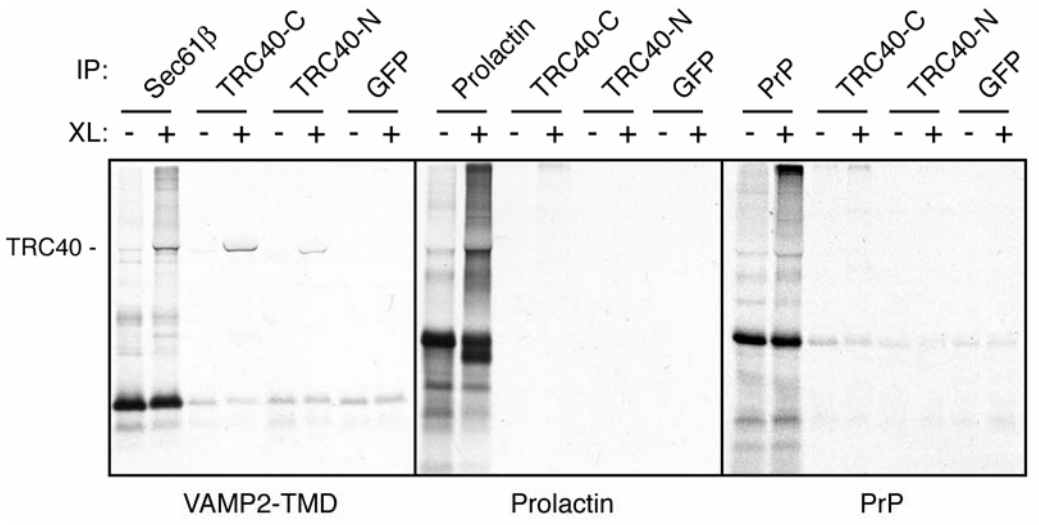

Figure S5. Analysis of various constructs for TRC40 interaction. The indicated constructs were tested for interaction with TRC40 by crosslinking and immunoprecipitation exactly as in Fig. 4A. The VAMP2-TMD construct shows crosslinks to TRC40 comparable to Sec61β, while neither Prolactin nor PrP showed any TRC40 crosslinking even upon overexposure of the autoradiographs. In a separate experiment, we found that Stx1-DN also showed crosslinking to TRC40 as seen for Sec61β (data not shown). It is worth noting that the negative crosslinking results in the case of Prolactin and PrP could formally be due to the lack of suitably positioned cysteines. We consider this possibility relatively unlikely because Prolactin has seven cysteines distributed throughout the protein and PrP has three (while Sec61β has only one). Also, the dominant-negative TRC40 has no effect on either Prolactin or PrP translocation, independently arguing against an interaction. And finally, the context-dependent effects seen in Fig. 4 show that even in instances where the number and positions of cysteines are the same, differences in TRC40 interactions are seen.

Supplementary References

Abell, B. M., Pool, M. R., Schlenker, O., Sinning, I., and High, S. (2004). Signal recognition particle mediates post-translational targeting in eukaryotes. Embo J *23*, 2755-2764.

Brambillasca, S., Yabal, M., Soffientini, P., Stefanovic, S., Makarow, M., Hegde, R. S., and Borgese, N. (2005). Transmembrane topogenesis of a tail-anchored protein is modulated by membrane lipid composition. Embo J *24*, 2533-2542.

Fons, R. D., Bogert, B. A., and Hegde, R. S. (2003). Substrate-specific function of the translocon-associated protein complex during translocation across the ER membrane. J Cell Biol *160*, 529-539.

Garrison, J. L., Kunkel, E. J., Hegde, R. S., and Taunton, J. (2005). A substrate-specific inhibitor of protein translocation into the endoplasmic reticulum. Nature *436*, 285-289.

Jackson, R. J., and Hunt, T. (1983). Preparation and use of nuclease-treated rabbit reticulocyte lysates for the translation of eukaryotic messenger RNA. Methods Enzymol *96*, 50-74.

Kutay, U., Ahnert-Hilger, G., Hartmann, E., Wiedenmann, B., and Rapoport, T. A. (1995). Transport route for synaptobrevin via a novel pathway of insertion into the endoplasmic reticulum membrane. Embo J *14*, 217-223.